

## Review

# Molecularly Imprinted Titanium Dioxide: Synthesis Strategies and Applications in Photocatalytic Degradation of Antibiotics from Marine Wastewater: A Review

Xue Han <sup>1</sup> , Yu Jin <sup>1</sup>, Luyang Zhao <sup>1</sup>, Yuying Zhang <sup>1</sup> , Binqiao Ren <sup>1,2,\*</sup> , Xiaoxiao Song <sup>1,\*</sup>  and Rui Liu <sup>3,\*</sup> 

<sup>1</sup> Institute of Advanced Technology, Heilongjiang Academy of Sciences, Harbin 150009, China; hxyep883@163.com (X.H.); jinyu36@126.com (Y.J.); zly516678@163.com (L.Z.); 18847008955@163.com (Y.Z.)

<sup>2</sup> Heilongjiang Institute of Environmental and Sciences, Harbin 150056, China

<sup>3</sup> Center of Pharmaceutical Engineering and Technology, Harbin University of Commerce, Harbin 150076, China

\* Correspondence: renbinqiao@126.com (B.R.); xiaoxiaosonggy@163.com (X.S.); liur@hrbcu.edu.cn (R.L.)

**Abstract:** Antibiotic residues in the marine environment pose a serious threat to ecosystems and human health, and there is an urgent need to develop efficient and selective pollution control technologies. Molecular imprinting technology (MIT) provides a new idea for antibiotic pollution control with its specific recognition and targeted removal ability. However, traditional titanium dioxide (TiO<sub>2</sub>) photocatalysts have limited degradation efficiency and lack of selectivity for low concentrations of antibiotics. This paper reviews the preparation strategy and modification means of molecularly imprinted TiO<sub>2</sub> (MI-TiO<sub>2</sub>) and its composites and systematically explores its application mechanism and performance advantages in marine antibiotic wastewater treatment. It was shown that MI-TiO<sub>2</sub> significantly enhanced the selective degradation efficiency of antibiotics such as tetracyclines and sulfonamides through the enrichment of target pollutants by specifically imprinted cavities, combined with the efficient generation of photocatalytic reactive oxygen species (ROS). In addition, emerging technologies such as magnetic/electric field-assisted catalysis and photothermal synergistic effect further optimized the recoverability and stability of the catalysts. This paper provides theoretical support for the practical application of MI-TiO<sub>2</sub> in complex marine pollution systems and looks forward to its future development in the field of environmental remediation.

**Keywords:** molecularly imprinted; TiO<sub>2</sub>; photocatalysis; antibiotics



Academic Editor: Steven L. Suib

Received: 3 April 2025

Revised: 4 May 2025

Accepted: 6 May 2025

Published: 7 May 2025

**Citation:** Han, X.; Jin, Y.; Zhao, L.; Zhang, Y.; Ren, B.; Song, X.; Liu, R. Molecularly Imprinted Titanium Dioxide: Synthesis Strategies and Applications in Photocatalytic Degradation of Antibiotics from Marine Wastewater: A Review. *Materials* **2025**, *18*, 2161. <https://doi.org/10.3390/ma18092161>

**Copyright:** © 2025 by the authors. Licensee MDPI, Basel, Switzerland. This article is an open access article distributed under the terms and conditions of the Creative Commons Attribution (CC BY) license (<https://creativecommons.org/licenses/by/4.0/>).

## 1. Introduction

In recent years, the development of efficient and selective pollutant degradation technologies has become a research hotspot as the problem of antibiotic pollution in the marine environment has become increasingly serious. Antibiotic wastewater enters the marine environment through industrial discharges, agricultural runoff, and atmospheric deposition, posing a serious threat to marine ecosystems and human health [1]. The World Health Organization (WHO) announced in 2019 that antimicrobial drug resistance is one of the top ten current threats to global health [2]. The overuse of antibiotics has led to the prevalence of antibiotic resistance. Global per capita antibiotic consumption in an estimated 76 countries was reported to have increased by 65% from 2000 to 2015 [3], and the COVID-19 pandemic has further exacerbated the problem of antibiotic misuse. Conventional treatment technologies (e.g., adsorption, biodegradation) have difficulty

coping with the complex challenges of high salinity and multi-pollutant coexistence in the marine environment, and, therefore, the development of novel degradation technologies combining high selectivity, resistance to interference, and environmental adaptability is imminent [4].

Molecular imprinting technology (MIT) can accurately construct spatially and chemically matched recognition sites with target pollutants through template molecular pre-assembly strategies [5] and has demonstrated unique advantages in the fields of sensing and separation, as shown in Figure 1 [6–14]. However, traditional molecularly imprinted polymers (MIPs) suffer from defects such as poor photostability and low mass-transfer efficiency, which limit their application in photocatalysis. For this reason, researchers have combined MIT with nanosemiconductor materials, among which  $\text{TiO}_2$  is an ideal carrier due to its high chemical stability, excellent photocatalytic activity, and low cost [15]. The molecularly imprinted  $\text{TiO}_2$  (MI- $\text{TiO}_2$ ) prepared by surface imprinting, sol-gel modification, and other strategies not only retained the efficient separation of photogenerated carriers of  $\text{TiO}_2$  but also could target enrichment of the target antibiotics in complex matrices by specifically recognizing the cavities, thus breaking the bottleneck of the efficiency of the traditional photocatalysis for low concentrations of pollutants [16].

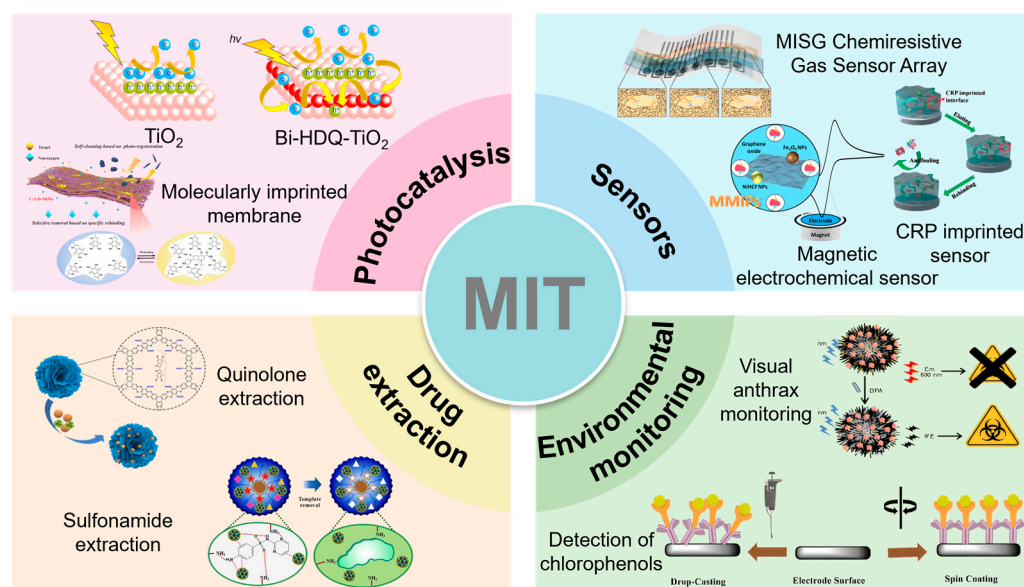


**Figure 1.** Application fields related to MIT [6–14].

This bifunctional synergistic mechanism of “molecular recognition-photocatalytic oxidation” has demonstrated unique advantages in marine pollution management; for example,  $\text{TiO}_2$ -functionalized biochar composites developed by Louros et al. were able to significantly improve the efficiency of photocatalytic degradation of sulfadiazine in mariculture wastewater [17]; Qin et al. designed  $\text{Fe}_3\text{O}_4@\text{TiO}_2$ -type magnetic molecularly imprinted nanoparticles for efficient and selective adsorption of chloramphenicol in high-salt marine sediments, with recoveries of 77.9–102.5% [18]. The above case validates the engineering potential of MI- $\text{TiO}_2$  in complex marine environments. In this paper, the synthesis strategy of MI- $\text{TiO}_2$  and its performance optimization mechanism in marine antibiotic degradation are systematically reviewed, focusing on the influence of modification means such as heterogeneous structure building, elemental doping, and photo-thermal synergism on the photocatalytic performance, and summarizing the removal effect of MI- $\text{TiO}_2$  on various types of antibiotics with the aim of providing theoretical support for the engineering application of MI- $\text{TiO}_2$ .

## 2. Sources and Characterization of Antibiotics in the Marine Environment

### 2.1. Sources of Marine Antibiotics

Land-based inputs are the main sources of antibiotics in the marine environment, mainly including aquaculture, agricultural activities, the pharmaceutical industry, medical wastewater, and domestic sewage. In aquaculture, antibiotics are widely used for the prevention and treatment of diseases in aquatic organisms and enter rivers or coastal waters through aquaculture wastewater discharged into sewage treatment sites [19]. In agricultural activities, antibiotics enter rivers through agricultural runoff and soil infiltration and eventually enter into the ocean [20]. Pharmaceutical industry wastewater contains high concentrations of antibiotic residues, even up to  $\text{mg}\cdot\text{L}^{-1}$  of antibiotics in the wastewater discharged by certain companies, which enter the ocean through rivers after treatment [21]. Antibiotics in medical wastewater enter the sewage system through patient excretion, and some residual drugs enter the water body after treatment, and medical wastewater contains more than 25% antibiotics compared to other wastewater [22]. Antibiotic metabolites from domestic wastewater may also enter the marine environment through the sewage system, and this type of wastewater contains the largest number and variety of microorganisms, which increases the emergence of drug-resistant organisms [23]. Existing antibiotic treatment processes have been reported to remove only 36–79% of antibiotics, and residual antibiotics enter the surface water environment through wastewater treatment plant outfalls and ultimately into bays and nearshore environments, which puts tremendous pressure on the marine ecosystem [24].

Atmospheric deposition is another important pathway for antibiotics to enter the oceans and includes both atmospheric wet deposition and atmospheric dry deposition. Atmospheric wet deposition refers to the entry of antibiotics into the atmosphere through aerosols or particulate matter, and then into the marine environment along with rainfall (e.g., rain, snow). Atmospheric dry deposition, on the other hand, involves antibiotics attaching to atmospheric particulate matter and settling directly on the ocean surface by gravity [25]. Both of these methods allow antibiotics to be transported from long distances and enter the ocean, further expanding the scope of their contamination.

Marine inputs mainly include mariculture wastewater and near-shore sewage discharges. In mariculture, antibiotics are used directly in aquaculture waters, and some drug residues are discharged into the ocean through wastewater. Industrial wastewater, domestic sewage, and ship discharges from near-shore areas may also contain antibiotic residues that enter the marine environment directly. These sources make antibiotics widely distributed in the near-shore and pelagic environments, posing a potential threat to marine ecosystems [26].

Antibiotic contamination in the marine environment is a complex multi-source problem (Figure 2), and together these sources contribute to the widespread distribution of antibiotics in the marine environment, posing a serious threat to marine ecosystems and human health [27]. The levels of antibiotics in marine environments around the world are shown in Table 1. Antibiotics are prevalent in marine environments, with sulfonamides and macrolides being the most commonly detected antibiotics (concentrations ranging from 0.3 to  $16,000\text{ ng}\cdot\text{L}^{-1}$ ), and there are differences in the types of antibiotics and the concentration levels of antibiotics detected in different places, which may be related to the local socioeconomic development level [28]. Therefore, strict control of antibiotic sources and the development of efficient treatment technologies are key to solving the problem of marine antibiotic pollution.

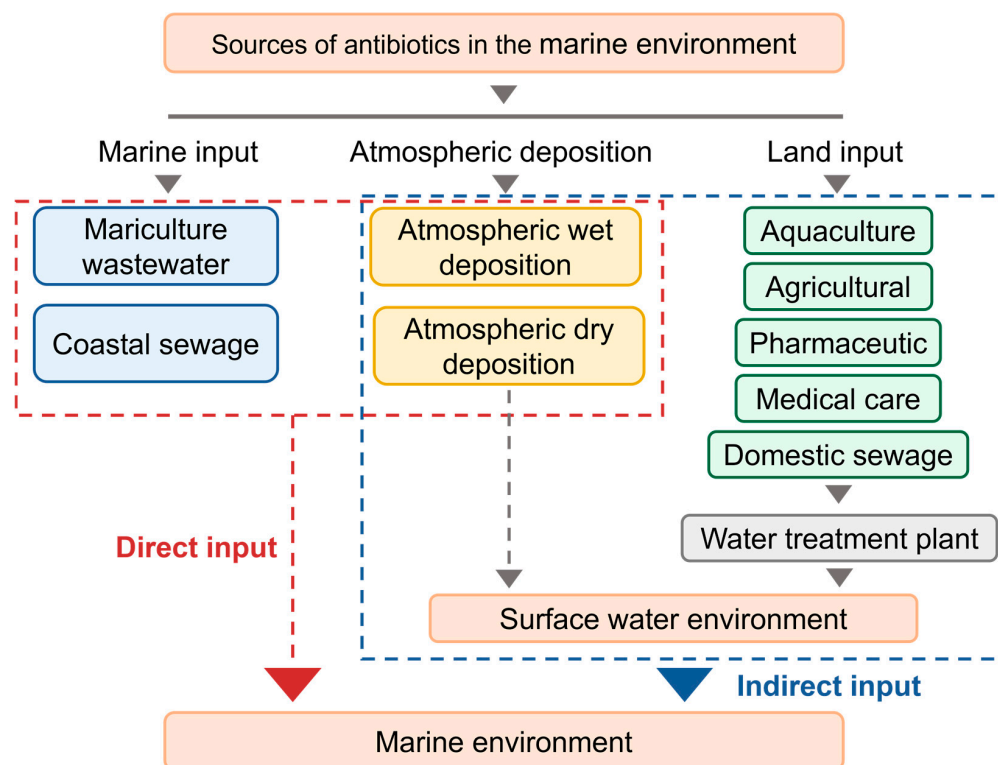


**Figure 2.** Sources of antibiotics in the marine environment.

**Table 1.** Levels of antibiotics in the marine environment worldwide.

Sea (Country)	Antibiotic	Concentration (ng·L <sup>-1</sup> )	Reference
Beibu Gulf (China)	Sulfamethoxazole	0–15.9	[29]
	Trimethoprim	0–4.11	
	Erythromycin	2.59–47.6	
Bohai Bay (China)	Tetracyclines	41.5–222.4	[30]
	Demeclocycline	276 ± 71.6	
Maowei Sea (China)	Norfloxacin	1.56 ± 1.46	[31]
	Enrofloxacin	0.85 ± 0.65	
Hailing Island (south coast of England)	Oxytetracycline	0–16,000	[32]
	Trimethoprim	0–20	
North coast of the Persian Gulf (Iran)	Norfloxacin	1.21–51.5	[33]
Baltic Sea (Northern Europe)	Sulfamethoxazole	0–311	[34]
	Trimethoprim	0–279	
Po Valley (Italy)	Clarithromycin	0–128.1	[35]
	Ciprofloxacin	0–124	
Cadiz Bay (Spain)	Azithromycin	0–1.2	[36]
	Erythromycin	0–0.3	
South Sea (Korea)	Norfloxacin	0–0.5	[37]
	Lincomycin	0–438	
Red Sea (Saudi Arabia)	Sulfamethoxazole	31.5–62.4	[38]
	Metronidazole	51.0–178.6	
Eastern Mediterranean (Greece)	Clarithromycin	0–1.5	[39]
	Amoxicillin	0–127.8	
Chesapeake Bay (United States)	Azithromycin	0–2.7	[40]
	Norfloxacin	0–94.1	

## 2.2. Characteristics of Marine Antibiotics

Antibiotics in the marine environment are a class of organic compounds with complex chemical structures. They usually contain functional groups such as hydroxyl, amino, and carboxyl groups. These groups not only give them biological activity but also significantly affect their migration and transformation behavior in the aquatic environment. The physicochemical properties of different types of antibiotics are significantly different; for example, tetracycline antibiotics are prone to photolysis due to their high water solubility and photosensitivity, while sulfonamide antibiotics can remain in the environment for a long time due to their strong chemical stability [41]. In addition, antibiotics in the environment make it easy to generate more toxic or more difficult to degrade intermediates (e.g., nitro or halogenated derivatives) through hydrolysis, oxidation, and other reactions, and their persistence and bioaccumulation pose multiple threats to marine ecosystems and human health. It is worth noting that the particularity of the marine environment further aggravates the difficulty of antibiotic removal; high salinity (e.g.,  $\text{Cl}^-$ ,  $\text{SO}_4^{2-}$ ) may inhibit the exposure of catalytic active sites through an ion shielding effect or compete with antibiotics for adsorption; coexisting pollutants (e.g., heavy metals, microplastics, and petroleum hydrocarbons) not only interfere with the targeted identification of antibiotics but also may amplify ecological risks through synergistic toxic effects [42].

## 2.3. Traditional Methods of Antibiotic Removal

Conventional treatment methods for antibiotic pollution in the marine environment mainly include physical, chemical, and biological technologies, but each has significant limitations. Although physical methods such as adsorption (activated carbon, clay, etc.) and membrane filtration (nanofiltration, reverse osmosis) can effectively retain antibiotics, they only achieve pollutant transfer rather than degradation and face difficulties in adsorbent regeneration, membrane fouling, and high energy consumption [43]. In chemical methods, although advanced oxidation processes (such as Fenton oxidation and ozone oxidation) can degrade antibiotics through reactive oxygen species (ROS), they often require harsh reaction conditions (e.g., specific pH) and may produce toxic by-products (e.g., halogenated compounds) [44]. Chlorination disinfection is widely used, but it is easy to produce more toxic chlorinated derivatives. Biodegradation depends on the activity of specific microorganisms or enzymes, but its efficiency is limited in high-salt and low-temperature marine environments and may accelerate the spread of antibiotic resistance genes (ARGs) [45]. In contrast, photocatalytic technology (especially  $\text{TiO}_2$ -based materials) shows significant advantages; it mineralizes antibiotics into  $\text{CO}_2$ ,  $\text{H}_2\text{O}$ , and harmless intermediates through photogenerated ROS (e.g.,  $\cdot\text{OH}$ ,  $\cdot\text{O}_2^-$ ), which is both efficient and environmentally friendly [46]. The characteristics of solar energy drive reduced energy consumption, in line with the principle of green chemistry; through functional modification such as element doping and heterostructure construction, it can adapt to high-salt or turbid seawater environments [47]. Moreover, MI- $\text{TiO}_2$  can achieve efficient degradation of antibiotics under low-concentration conditions, providing a new generation of solutions for marine antibiotic pollution control.

# 3. Preparation and Modification of Imprinted Titanium Dioxide Catalysts

## 3.1. Preparation Method

### 3.1.1. Surface Molecular Imprinting

Surface molecular imprinting is a more commonly used method that refers to an imprinting technique in which a polymerization reaction occurs on the surface of a carrier, such as a chemically modified silica gel or metal oxide, so that the molecularly imprinted recognition sites are distributed on the surface of the molecularly imprinted polymer or solid-phase matrix. Combining the ability of  $\text{TiO}_2$  photocatalytic degradation of organic



pollutants and the ability of molecularly imprinted polymers to recognize organic pollutants exclusively, by selecting suitable functional monomers and template molecules, and then adding cross-linking agents and titanium sources as precursors, specific pores were formed on the surface of  $\text{TiO}_2$  through chemical polymerization reactions to generate pre-polymerized complexes, which can achieve selective degradation of high-toxicity and low-concentration pollutants (Figure 3) [48]. The molecular imprinting on the  $\text{TiO}_2$  surface, on the one hand, can expose the molecular recognition sites on the  $\text{TiO}_2$  surface and improve the mass transfer between the recognition sites and the target molecules; on the other hand, the template molecules are easy to be eluted completely, and it is favorable for the recombination between the recognition sites and the template molecules. In addition, the catalytic performance of the composites can be improved by adjusting the synthesis parameters, such as reaction time, temperature, and pH value, so that the composites can perform more efficiently and persistently in the treatment of low concentrations of highly toxic organic pollutants. Li et al. [49] used surface molecularly imprinted technology to prepare  $\text{TiO}_2/\text{SiO}_2$  hybrid fibers by adding templates to the precursor solution, with titanate-butyl ester (TBOT) as the titanium source, and the functional monomer binds to rhodamine B (RhB) and generates specific recognition sites, and the imprinted fibers exhibit higher adsorption capacity and selectivity compared to the non-imprinted samples. He et al. [50] prepared magnetic molecularly imprinted nanocomposites by surface imprinting, which were capable of dispersive solid-phase extraction of doxycycline from marine sediments with a low detection limit ( $0.03 \mu\text{g}\cdot\text{g}^{-1}$ ) and excellent recoveries (90.60~93.76%). Li et al. [51] prepared molecularly imprinted  $\text{Ag}_3\text{PO}_4/\text{TiO}_2$  photocatalysts (MATs) using sulfadimethoxine as a template and TBOT as a functional monomer, and the MAT surfaces formed distinct imprinted cavities and n-p-type heterojunctions on the surface of MAT and had a large specific surface area, and the degradation rate of sulfadimethoxine reached 82.4%.

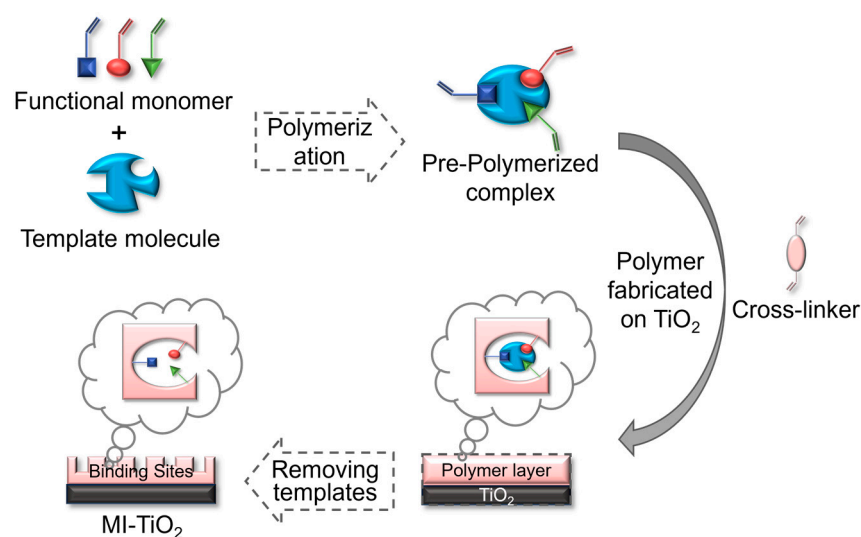


**Figure 3.** Synthesis process of surface MI- $\text{TiO}_2$  [48].

### 3.1.2. Molecularly Imprinted Sol-Gel Technology

The molecularly imprinted sol-gel technique is a method of introducing template molecules into an inorganic network structure through a sol-gel process, which elutes to form a rigid material. This technique combines the advantages of the sol-gel method, such as mild preparation conditions, modulation of the average pore size, pore distribution, and specific surface area of the material, while overcoming the shortcomings of traditional molecularly imprinted organic polymers that are less rigid and inert [52]. Therefore, molec-

ularly imprinted sol-gel technology has become an important direction of current research, providing a new way for the preparation of high-performance molecularly imprinted materials. Huang et al. [53] synthesized a novel photocatalyst (MIP-Nd-TiO<sub>2</sub>) by the sol-gel method and optimized the preparation conditions by adjusting the doping amount of Nd, calcination conditions, and so on, which resulted in the degradation of oxytetracycline (OTC) by up to 91.97%. Ferreira et al. [54] used titanium isopropoxide (TTIP) and methyl-triisopropoxide titanium (MTTIP) as precursors to synthesize methyl-modified hollow TiO<sub>2</sub> microspheres with selectivity by the sol-gel method and obtained a certain degree of mixed-network organization, which increased with the calcination temperature.

### 3.1.3. Other Methods

In addition to the above methods, molecularly imprinted TiO<sub>2</sub> is also prepared by the hydrothermal method and liquid phase deposition method. The hydrothermal method forms molecularly imprinted TiO<sub>2</sub> materials with specific pore structures by reacting titanium source precursors with template molecules and functional monomers in a high-temperature and -pressure hydrothermal environment using water as the reaction medium [55]. The materials prepared by this method usually have high crystallinity and stability, and the morphology and properties of the materials can be further optimized by adjusting the parameters, such as hydrothermal temperature, time, and pH. Xiong et al. [56] prepared a novel electrochemical sensor (MIPs/TiO<sub>2</sub> NRAs@FTO) for the detection of salicylic acid by the hydrothermal method. The nanorod structure of TiO<sub>2</sub> for SA provided high specific surface area, increased imprinting sites, improved internal mass transport, and enhanced the accessibility of the active sites, thus improving the sensitivity and binding ability of the sensor. Liquid phase deposition is a technique to deposit TiO<sub>2</sub> thin films on the substrate surface by chemical reaction in solution at room temperature or low temperature. This method is simple, low-cost, and enables precise regulation of film thickness and structure. Li et al. [57] used the sol-gel method combined with the liquid phase deposition technique to prepare iron-doped TiO<sub>2</sub>/SiO<sub>2</sub> (Fe@TS) nanofibrous membranes with molecularly imprinted modification, and the composites formed a thin layer of molecularly imprinted polymers in liquid phase, and 4-nitrophenol's photodegradation showed excellent selectivity.

## 3.2. Modification Method

Conventional TiO<sub>2</sub> suffers from a narrow photoresponse range, high photogenerated carrier complexation rate, and poor selectivity to target pollutants, which limit its practical applications. To overcome these limitations, researchers have optimized molecularly imprinted TiO<sub>2</sub> through various modification methods, including elemental doping, composite structure construction, morphology modulation, surface functionalization, photochemical synergistic effect, and magnetic/electric field-assisted catalysis [58].

### 3.2.1. Elemental Admixture

Elemental doping is used to enhance photocatalytic efficiency by introducing metallic or non-metallic elements into the TiO<sub>2</sub> lattice to modulate its electronic structure and light absorption properties. Metal doping (e.g., Fe, Cu, Ag, etc.) introduces impurity energy levels and promotes the separation of photogenerated electron-hole pairs while broadening the photoresponse of TiO<sub>2</sub> to the visible region. Uthiravel et al. [59] prepared Ag-doped TiO<sub>2</sub> nanoparticle photocatalysts by the co-precipitation method, and the Ag doping significantly reduced the band gap of TiO<sub>2</sub> (3.3 eV for TiO<sub>2</sub>, 0.9 eV for Ag-TiO<sub>2</sub>), and the degradation of methylene blue by Ag-TiO<sub>2</sub> under light was as high as 96.96%. Non-metal doping (e.g., N, C, S, etc.), on the other hand, enhances the light absorption ability of TiO<sub>2</sub> under visible light by lowering its bandgap. Kuang et al. [60] proposed an

N-doped TiO<sub>2</sub>/Ti<sub>3</sub>C<sub>2</sub> heterojunction-driven auto-photocatalytic platform for the detection of dexamethasone (DXM), where N doping promotes the conversion of dissolved oxygen to H<sub>2</sub>O<sub>2</sub>, providing more co-reactants to enhance the electrical signal and making it so that the molecularly imprinted electrochemical sensor has a wide linear range ( $1.0 \times 10^{-6}$ – $1.0 \times 10^1$  µg·mL<sup>−1</sup>) and low detection limit. Elemental doping can effectively improve the photocatalytic activity of TiO<sub>2</sub> and enhance its ability to degrade the target pollutants, and the effects of different elemental doping on the photocatalytic performance of TiO<sub>2</sub> are shown in Table 2. These elemental doping strategies provide a new idea for the development of highly efficient and stable MI-TiO<sub>2</sub> photocatalysts, which is expected to promote its practical application in the treatment of marine antibiotic wastewater.

**Table 2.** Effect of doping with different elements on the photocatalytic performance of TiO<sub>2</sub>.

Element	Photocatalyst	Pollutant	Degradation (%)	Reference
Pr	Pr-MIP-TMCs	Dinitrophenol	92	[61]
Ni and F	Ni-F-TiO <sub>2</sub>	acetaminophen	84	[62]
P	0.071PT	<i>Escherichia coli</i>	90	[63]
Ag and Zn	Ag/Zn-MIP-TiO <sub>2</sub>	Ethyl hydroxybenzoate	99	[64]
Ce	Ce-TiO <sub>2</sub>	Tetracycline	86	[65]
K	TNT-K5	Methylene blue	97	[66]
La	La/TiO <sub>2</sub>	Cyanide	98	[67]
B	B-TiO <sub>2</sub>	Diclofenac sodium	98	[68]
Mg	Mg-doped TiO <sub>2</sub>	Methyl orange	95	[69]
V	(TiO <sub>2</sub> :V)/rGO	Rhodamine B	95	[70]
La and I	LICT	Methylene blue	98	[71]

### 3.2.2. Composite Structure Construction

Composite structure construction is carried out by combining TiO<sub>2</sub> with other materials (e.g., semiconductors, carbon materials) to form heterojunctions or composites to enhance its photocatalytic performance. Deng et al. [72] prepared TiO<sub>2</sub> NP/g-C<sub>3</sub>N<sub>4</sub> photocatalysts, and the heterojunction formed was able to inhibit the compounding of photogenerated electron–hole pairs effectively to improve the photocatalytic efficiency. Lin et al. [73] prepared composite photocatalysts using P25TiO<sub>2</sub> and graphene as raw materials to prepare a composite photocatalyst; graphene can broaden the range of photo-response of the material and improve its electrical conductivity, which can help to quickly transfer the electrons generated by the light excitation of TiO<sub>2</sub> and reduce the electron–hole pair compounding, thus enhancing the photocatalytic activity, and the experimental results showed that a 10 mg·L<sup>−1</sup> solution of methyl orange was able to be completely degraded within 12 min, which was 1.81 times that of TiO<sub>2</sub>. Ye et al. [74] prepared a CdS/TiO<sub>2</sub> composite photocatalyst using a ball milling process, which showed a photocatalytic degradation efficiency of 57.84% for methyl orange after 2 h of UV illumination. Qin et al. [75] prepared TiO<sub>2</sub>/BiYO<sub>3</sub> photocatalysts for water resolution of hydrogen, and the experimental results showed that the photocatalytic hydrogen precipitation rate was 10 times higher than that of TiO<sub>2</sub> and 57 times higher than that of BiYO<sub>3</sub>, respectively. Alimard et al. [76] synthesized Bi/BiOBr/TiO<sub>2</sub> composites by the solvothermal method, which showed high photocatalytic performance for NO and NO<sub>2</sub> under both visible and UV lamps. The composite structure can achieve efficient photocatalytic degradation by modulating the energy band structure and interfacial properties of the material (Table 3), providing a more efficient solution for environmental treatment and energy conversion.



**Table 3.** Effect of different composites on the photocatalytic performance of TiO<sub>2</sub>.

Material	Photocatalyst	Pollutant	Degradation (%)	Reference
CQDs	TiO <sub>2</sub> /CQDs	Methyl orange	85	[77]
LaFeO <sub>3</sub>	LaFeO <sub>3</sub> /TiO <sub>2</sub>	Methylene blue	96	[78]
Chitosan	TiO <sub>2</sub> /Chitosan	Gallic acid	81	[79]
MoS <sub>2</sub>	TiO <sub>2</sub> /MoS <sub>2</sub>	Oilfield suspended solids	93	[80]
FeOOH	FeOOH/TiO <sub>2</sub>	Rodamine B	84	[81]
Bi <sub>2</sub> O <sub>3</sub>	Bi <sub>2</sub> O <sub>3</sub> /brookite TiO <sub>2</sub>	Ofloxacin	91	[82]
BiPO <sub>4</sub>	TiO <sub>2</sub> /BiPO <sub>4</sub>	Kamasipin	88	[83]
Activated Charcoal	AC-TiO <sub>2</sub>	N-Acetyl-p-Aminophenol (APAP)	82	[84]
g-C <sub>3</sub> N <sub>4</sub>	g-C <sub>3</sub> N <sub>4</sub> -TiO <sub>2</sub> -Ag	Malachite green	66	[85]
ZnO and rGO	ZnO-TiO <sub>2</sub> /rGO	Methylene blue	100	[86]
MoS <sub>2</sub>	BC/MoS <sub>2</sub> /TiO <sub>2</sub>	Escherichia coli	100	[87]
Ag <sub>2</sub> CrO <sub>4</sub>	Ag <sub>2</sub> CrO <sub>4</sub> /TiO <sub>2</sub>	NO <sub>2</sub> <sup>−</sup>	100	[88]

### 3.2.3. Conformal Modification

Conformal modulation is used to optimize the photocatalytic performance of TiO<sub>2</sub> by designing its microstructure (e.g., nanotubes, nanosheets, nanospheres, etc.). Wu et al. [89] prepared TiO<sub>2</sub> nanotube (TiNT) arrays on titanium foil and synthesized TiO<sub>2</sub> nanotube arrays with a high specific surface area and ordered structure, which could provide more active sites and enhance the efficiency of photocatalytic reaction. Sharafudheen et al. [90] prepared porous TiO<sub>2</sub> nanomaterials using titanium isopropoxide as raw material, and the BET analysis results showed a specific surface area of 134 m<sup>2</sup>·g<sup>−1</sup>, and the excellent specific surface area increased the contact area between the reactants and the catalysts, which further enhanced the degradation effect. Liu et al. [91] prepared Ag/TiO<sub>2</sub> nanofibrous films, and the synthesized nanofibrous films with a larger specific surface area and more reaction sites were provided, and the degradation rate of rhodamine B reached 73%, which was much higher than that of TiO<sub>2</sub> particles. The morphology modification not only improved the physicochemical properties of TiO<sub>2</sub> but also enhanced its adsorption and degradation of target pollutants, providing an efficient catalyst for marine antibiotic wastewater treatment.

### 3.2.4. Surface Functionalization

Surface functionalization is the process of improving the surface properties of TiO<sub>2</sub> by introducing organic molecules or functional groups (e.g., carboxylic acids, amine groups, etc.) on its surface to enhance the selective adsorption and degradation of specific pollutants. Mendonça et al. [92] used ethylenediamine-modified activated carbon and impregnated it with TiO<sub>2</sub> to prepare a novel absorbent/photocatalyst material (AC-ET/TiO<sub>2</sub>), and the insertion of amine groups enhanced the stability of the TiO<sub>2</sub> surface for rapid degradation of sulfadimethazine. Wu et al. [93] successfully synthesized six functional conjugated microporous polymers (CMPs) containing amino, hydroxyl, carboxyl, and ester groups via the Sonogashira–Hagihara coupling reaction and uniformly encapsulated TiO<sub>2</sub> on the surface of the CMPs under solvent-heated conditions. Due to the high electronegativity of the carboxyl group, The CMP/TiO<sub>2</sub> containing carboxyl groups showed the smallest band gap, the highest photocurrent intensity, and the lowest electrical resistance, which significantly improved the photocatalytic activity. Wang et al. [94] prepared an acid-induced assembly of rutile TiO<sub>2</sub> photocatalysts by treating layered protonated titanates using a concentrated HNO<sub>3</sub> solution. The experimental results showed that nitrate grafting made the surface of rutile TiO<sub>2</sub> negatively charged, which was conducive to the capture of positive protons and improved carrier separation, thus enhancing photocatalytic hydrogen production. The surface functionalization not only improves the selectivity of TiO<sub>2</sub> but also

optimizes its interaction with the target pollutants, enabling it to exhibit higher catalytic efficiency in complex wastewater systems.

### 3.2.5. Photothermal Synergy

The photothermal synergistic effect is achieved by compounding  $\text{TiO}_2$  with photothermal materials (e.g., carbon-based materials, metal sulfides), which utilizes the photothermal effect to enhance the local temperature and accelerate the reaction kinetics. Li et al. [95] successfully prepared black  $\text{TiO}_2/\text{MoS}_2/\text{Cu}_2\text{S}$  hierarchical tandem heterojunction visible light photocatalysts with a mesoporous structure by evaporation-induced self-assembly, high-temperature hydrogenation, and solvent-thermal method, which can effectively absorb near-infrared energy to enhance the photothermal effect, and the narrow bandgap properties of  $\text{MoS}_2$  and  $\text{Cu}_2\text{S}$  can efficiently convert sunlight into heat, thus significantly enhancing the photocatalytic performance. Yang et al. [96] prepared photothermally coupled  $\text{TiO}_2/\text{BiS}$  S-type heterojunction nanofibers for photothermally catalyzed  $\text{CO}_2$  reduction, and the excellent photothermal conversion ability of BiS enabled the heterogeneous photocatalysts to accelerate the photogenerated electron transfer rate, and surface reaction rates were further accelerated, which were 5.24 times higher than those of the pristine  $\text{TiO}_2$ . Su et al. [97] designed MOF-derived C/ $\text{TiO}_2$  composites with simultaneous photothermal and photocatalytic functions for wastewater purification, and the materials possessed excellent sunlight absorptivity and superhydrophilicity, a large specific surface area, and a porous structure and degraded bottom organic pollutants in the water by up to 92.75%. The photothermal synergistic effect not only enhances the photocatalytic performance of  $\text{TiO}_2$  but also improves its applicability in complex wastewater systems, which provides a new idea for the treatment of marine antibiotic wastewater.

### 3.2.6. Magnetic/Electric Field-Assisted Catalysis

Magnetic/electric field-assisted catalysis is the enhancement of photocatalytic performance by compositing  $\text{TiO}_2$  with magnetic materials (e.g.,  $\text{Fe}_3\text{O}_4$ ) using an applied magnetic or electric field. Tang et al. [98] successfully achieved efficient photocatalytic degradation of tetracycline over  $\text{Ag}_2\text{S}/\text{TiO}_2$  catalysts using an external magnetic field-assisted strategy due to the fact that the Lorentzian force of an external magnetic field acting on charge carriers can promote the photogenerated carrier separation, which further enhances the catalytic effect. Grzegórska et al. [99] prepared a  $\text{TiO}_2/\text{Ti}_3\text{C}_2/\text{MnFe}_2\text{O}_4$  magnetic photocatalyst, which was able to completely degrade carbamazepine and ibuprofen under simulated sunlight with PMS-assisted photo-degradation in 20 min and could be magnetically separated by an external magnetic field after the degradation process. In Gu et al. [100], Z-type  $\text{WO}_3/\text{TiO}_2$  heterojunction catalysts were successfully prepared by an impregnation sintering process, and 98% degradation was achieved at an initial dichloromethane concentration of 200 ppm, and the excellent performance was mainly attributed to the built-in electric field and narrower bandgap, which effectively reduced the electron and hole complexation and thus increased the generation of more reactive oxygen species. The magnetic/electric field-assisted catalysis not only improves the catalytic performance of  $\text{TiO}_2$  but also enhances its maneuverability and cyclic stability in practical applications, providing an efficient and sustainable solution for marine antibiotic wastewater treatment.

As shown in Table 4, morphology modification, surface functionalization, photothermal synergy, and magnetic/electric field-assisted catalytic modification strategies can significantly improve the catalytic activity of  $\text{TiO}_2$ , with breakthroughs in photodegradation efficiency, target selectivity, and energy conversion performance. However, the high salinity of the marine environment, the coexistence of multiple pollutants, and the cost con-

straints of engineering applications require the optimization of the modification schemes for specific scenarios in order to promote large-scale applications. It should be noted that each modification strategy has significant limitations while enhancing the performance (Table 5), which should be balanced and optimized according to actual needs.

**Table 4.** Effects of different modification methods on the photocatalytic performance of TiO<sub>2</sub>.

Method	Photocatalyst	Target Substance	Photocatalytic Performance	Reference
Conformal modification	CR- TiO <sub>2</sub> NPs	Phenol red	Degradation rate 94%	[90]
	Ag/TiO <sub>2</sub> nanofiber film	Rhodamine B	Degradation rate 73%	[91]
Surface functionalization	AC-ET/90TiO <sub>2</sub>	Sulfadimethoxine	Degradation rate 90%	[92]
	CMP/TiO <sub>2</sub>	Ciprofloxacin	Degradation rate 97%	[93]
	Rutile TiO <sub>2</sub>	Hydrogen production	Hydrogen precipitation rate 402 $\mu\text{mol}\cdot\text{h}^{-1}$	[94]
Photothermal Synergy	TiO <sub>2</sub> /MoS <sub>2</sub> /Cu <sub>2</sub> S	Hydrogen production	Hydrogen precipitation rate 3377 $\mu\text{mol}\cdot\text{h}^{-1}$	[95]
	TiO <sub>2</sub> /BiS	CO <sub>2</sub> reduction	Reduction rate 8 $\mu\text{mol}\cdot\text{h}^{-1}$	[96]
Magnetic/Electric field assisted catalysis	UiO-66-NH <sub>2</sub> (Ti)	Methyl orange	Degradation rate 93%	[97]
	Ag <sub>2</sub> S/TiO <sub>2</sub>	Tetracycline	Degradation rate 96%	[98]
	TiO <sub>2</sub> /Ti <sub>3</sub> C <sub>2</sub> /MnFe <sub>2</sub> O <sub>4</sub>	Ibuprofen	Degradation rate 100%	[99]
	WO <sub>3</sub> /TiO <sub>2</sub>	Dichloromethane	Degradation rate 98%	[100]

**Table 5.** Advantages and disadvantages of different modification methods.

Modification Method	Advantages	Disadvantages	Reference
Element doping	High carrier separation efficiency; high selectivity	Doping amount is difficult to control; high cost	[101]
Composite structure construction	Versatility; high stability	Complicated preparation process; difficult to recover	[102]
Conformal modification	High surface area; strong adsorption properties	Difficult preparation; poor structural stability	[103]
Surface functionalization	High selectivity; high dispersibility	Poor modification stability; side reactions	[104]
Photothermal synergistic effect	High reaction rate; strong light absorption	High energy consumption; high material cost	[105]
Magnetic/electric field assisted catalysis	High separation and recovery; high reaction efficiency	High energy consumption; limited scope of application	[106,107]

#### 4. Application of Imprinted Titanium Dioxide in Antibiotic Degradation

In recent years, antibiotic pollution has become a hot issue studied by scholars from various countries, especially the fact that only 15% of antibiotic drugs will be absorbed and utilized, and the rest will be directly discharged into the ecosystem in the form of prodrugs, which has a very serious impact on the environment [108]. In addition, antibiotics are characterized by many interfering factors and low residues, so it is very important to choose a suitable treatment method [109]. MI-TiO<sub>2</sub> photocatalytic degradation of antibiotics is an efficient technology for environmental treatment. Its mechanism is based on the catalyst design of molecular imprinting technology, which can selectively recognize and adsorb specific antibiotic molecules to achieve antibiotic degradation efficiency under low-concentration conditions [110]. Common antibiotics, as shown in Figure 4, are mainly classified into tetracyclines (e.g., tetracycline, oxytetracycline), sulfonamides (e.g., sulfamethoxazole, sulfadiazine), quinolones (e.g., ciprofloxacin, norfloxacin), macrolides (e.g., erythromycin, azithromycin), and  $\beta$ -lactams (e.g., penicillin, cephalosporin). The degradation mechanism can be summarized as follows (Figure 5): (1) molecularly imprinted cavities target the

adsorption of target antibiotics and enrich the pollutants through specific interactions (e.g., hydrogen bonding, electrostatic, or hydrophobic interactions); (2) photoexcitation of  $\text{TiO}_2$  generates electron–hole pairs, generating reactive oxygen species (ROS) such as hydroxyl radicals ( $\cdot\text{OH}$ ) and superoxide radicals ( $\cdot\text{O}_2^-$ ), which leads directly to oxidative degradation of antibiotic molecules [111,112]. The imprinted cavity can effectively inhibit the photogenerated carrier complexation and prolong the contact time between the active species and the pollutants, thus improving the catalytic efficiency, which is divided into the following studies for the degradation of five types of typical antibiotics.

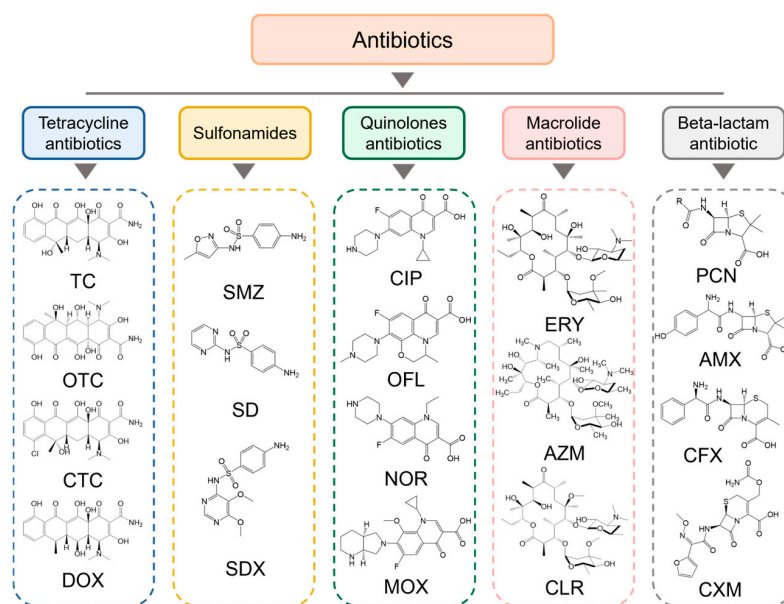


**Figure 4.** Antibiotics commonly found in the marine environment.

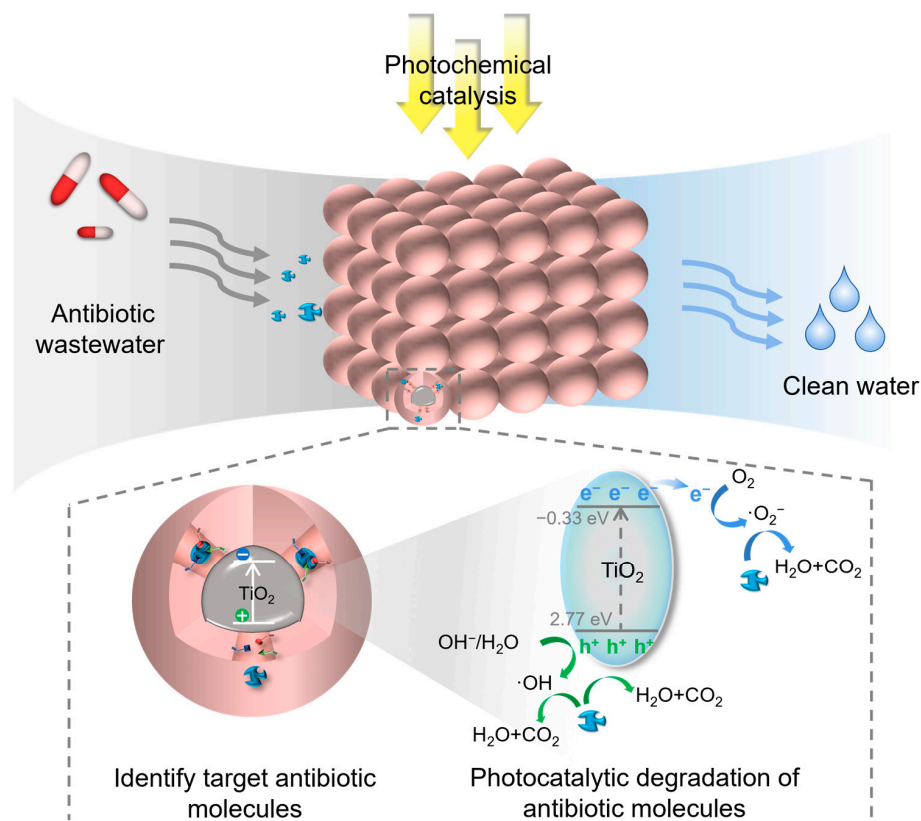


**Figure 5.** Mechanism of antibiotic degradation by MI- $\text{TiO}_2$ .

#### 4.1. Tetracycline Antibiotics

Tetracycline antibiotics (TCs) are difficult to be effectively degraded by conventional processes due to the chemical inertness of their benzotetracycline rigid skeleton. MI-TiO<sub>2</sub> significantly enhanced the selective capture of trace tetracycline antibiotics by precisely designing the imprinted cavities matching the hydroxyl and amide groups of the tetracycline antibiotics. Li et al. [113] combined the Stöber method with the sol-gel method and successfully constructed the molecularly imprinted molecules with core-shell structure TiO<sub>2</sub> (MIP-TiO<sub>2</sub>@SiO<sub>2</sub>), whose imprinting sites were highly compatible with the molecular conformation of tetracycline, and the degradation rate of tetracycline reached 82.18% under 60 min visible light irradiation. Huang et al. [53] optimized the energy bands of the MIP-Nd-TiO<sub>2</sub> catalyst energy band structure; the degradation rate of oxytetracycline was as high as 91.97% under simulated sunlight, and the degradation pathway was revealed by LC-MS analysis:  $\beta$ -keto group demethylation  $\rightarrow$  aromatic ring breakage  $\rightarrow$  final mineralization to CO<sub>2</sub> and H<sub>2</sub>O. The surface-imprinted photocatalyst (TMIP) developed by Fu et al. [114] effectively overcame the constraints of reaction kinetics. Under visible light irradiation, complete tetracycline degradation was achieved within 20 min ( $k = 0.153 \text{ min}^{-1}$ ), with a selectivity coefficient for tetracycline antibiotics ( $\alpha = 3.367$ ) significantly exceeding those for ciprofloxacin (2.389) and sulfonamide pollutants ( $<1.2$ ). These results confirm that the conformationally-matching imprinted cavities selectively enhance tetracycline degradation through structural recognition. Fu et al. [115] prepared an efficient composite photocatalyst by adjusting the doping ratios of different metal ions, and the degradation efficiency of tunicamycin in mariculture wastewater was as high as 73.04%. Guo et al. [116] used a Si-doped molecularly imprinted material prepared by liquid phase deposition method (TiO<sub>2</sub>/SiO<sub>2</sub>/OTC), which showed 80.79% degradation of oxytetracycline under 120 min xenon lamp irradiation through the domain-limiting effect of the SiO<sub>2</sub> mesoporous structure and the synergistic effect of charge transfer by the Si-O-Ti bonds, and the activity was stabilized after several cycles. These studies provide theoretical and technological paradigms for the targeted identification and efficient mineralization of tetracycline antibiotics in complex water bodies.

#### 4.2. Sulfonamide Antibiotics

Sulfonamide antibiotics (SAs) possess broad-spectrum antimicrobial properties due to their sulfonamide moiety and p-aminobenzene ring structure, but the chemical inertness of their aromatic rings and the high stability of their sulfonamide bonds lead to persistent residues in the environment, which aggravate the ecological risks. In order to break through this bottleneck, researchers have developed highly efficient targeted degradation systems by molecularly imprinted technology. Li et al. [117] systematically prepared four molecularly imprinted photocatalysts (MIP-TiO<sub>2</sub>/SD, MIP-TiO<sub>2</sub>/SMZ, MIP-TiO<sub>2</sub>/SN, and MIP-TiO<sub>2</sub>/AN) and found that the selective degradation efficiencies of sulfadiazine and sulfamethoxazole differed significantly from those of sulfonamide and sulfamethoxazole. The selective degradation efficiencies differed significantly, and the following common degradation pathways of sulfonamide antibiotics were revealed by intermediates analysis: single bond breaking, hydroxyl radical ( $\cdot\text{OH}$ ) mediated ring-opening reaction, and oxidative removal of amino groups. Wang et al. [118] constructed an Fe-doped molecularly imprinted photocatalyst (SA-Fe@TiO<sub>2</sub>) in one step, with photogenerated holes ( $h^+$ ),  $\cdot\text{OH}$ , and superoxide radicals ( $\cdot\text{O}_2^-$ ) synergistically enhancing the sulfamethoxazole degradation rate by 4.3-fold compared with pure TiO<sub>2</sub>, while exhibiting excellent ability to inactivate antibiotic resistance genes, significantly reducing the risk of environmental drug resistance spread. Zhang et al. [119] designed a novel ternary composite catalyst (MFTC, TiO<sub>2</sub>@Fe<sub>2</sub>O<sub>3</sub>@g-C<sub>3</sub>N<sub>4</sub>) whose molecularly imprinted cavity's ability to target captured



sulfamethoxazole resulted in a degradation rate up to twice that of similar pollutants and stable performance after several cycles. These studies deepened the mechanism of selective photocatalytic degradation of sulfonamide antibiotics from molecular recognition/active site modulation/interfacial charge separation in a multi-dimensional way, which provides a new idea for the precise management of sulfonamide pollutants in complex water bodies.

#### 4.3. Quinolone Antibiotics

The fluoroquinolone structures of quinolone antibiotics (QNs) have strong antimicrobial activity, but their chemical stability increases the difficulty of environmental degradation. Researchers have developed several efficient degradation strategies by molecular imprinting technology (MIT). Li et al. [120] prepared TiO<sub>2</sub>-loaded carbon nanosheet composites using ciprofloxacin as a template molecule. The material significantly enhanced the targeted degradation efficiency of quinolone antibiotics at low concentrations through the synergistic effects of the specific recognition of molecularly imprinted cavities, the adsorption enhancement of the carbon matrix material, and the photocatalytic activity of TiO<sub>2</sub>, with an adsorption selectivity coefficient of 7.2 and a photocatalytic selectivity coefficient of 3.2 for ciprofloxacin. Qin et al. [121] used molecularly imprinted polymers for the selective detection of norfloxacin in seawater, with detection limits of 2 µg·L<sup>-1</sup> and 5 µg·kg<sup>-1</sup> in seawater samples and sediments, respectively. Zheng et al. [122] further designed a mesoporous TiO<sub>2</sub>-based inorganic molecularly imprinted magnetic photocatalyst (MIFTA) whose unique pore structure and magnetic components endowed the material with high selectivity (norfloxacin adsorption capacity of 135.7 µg·mg<sup>-1</sup>, which was 1.4–2.3 times higher than that of conventional catalysts) and convenient recyclability (magnetic separation efficiency > 95%). In addition, Li et al. [123] modified commercial TiO<sub>2</sub> particles (P25) with a surface molecular imprinting technique, and the resulting imprinted material showed significantly better adsorption capacity for norfloxacin than non-imprinted material and pristine P25, and the removal efficiencies for structurally similar ciprofloxacin, carbamazepine, and phenol were 78.87%, 7.87%, and 2.68%, respectively, which sufficiently verified that molecularly imprinted sites are effective for fluoro quinolones by the specific affinity mechanism of molecularly imprinted sites. These studies provide important theoretical and technical support for the efficient and selective removal of quinolone antibiotics in complex water bodies.

#### 4.4. Macrolide Antibiotics

Macrolide antibiotics (MLs) can be efficiently bound to the specific cavities of MI-TiO<sub>2</sub> through intermolecular forces such as hydrophobic interaction, hydrogen bonding, and  $\pi$ - $\pi$  stacking. To address its environmental residue problem, Xie et al. [124] developed an erythromycin molecularly imprinted polymer (EMIP), which has a mesoporous structure (specific surface area of 265.62 m<sup>2</sup>·g<sup>-1</sup>, pore size of 2–5 nm) and hydrophobic surface properties, with an adsorption capacity of 4015.51 µg·g<sup>-1</sup> at an erythromycin concentration of 100 µg·L<sup>-1</sup> and adsorption efficiency remaining above 80% after five cycles. The retention of performance was >80%, attributed to the precise matching of the imprinted cavity to the erythromycin macrolide skeleton. In the field of photocatalytic degradation, Čizmić et al. [125] demonstrated a broad-spectrum applicability of TiO<sub>2</sub> nanofilms prepared by the over sol-gel method, evaluated the effects of different pH, aqueous substrate, drug coexistence, and radiation source factors on the degradation process and identified five azithromycin degradation products, none of which showed toxicity, suggesting the effective removal of azithromycin. Satulu et al. [126] counted a CA-GO-TiO<sub>2</sub>/PTFE composite membrane with a gradient pore structure, in which the polytetrafluoroethylene (PTFE) substrate successfully maintained the bulk porosity of the carrier while improving the ther-

mal and chemical stability of the membrane, and the degradation of azithromycin effluent was more than 80%, which provided a technical support for the large-scale treatment of macrolide antibiotics.

#### 4.5. $\beta$ -Lactam Antibiotics

$\beta$ -lactam antibiotics (BLs) exert potent antimicrobial effects through their characteristic  $\beta$ -lactam ring; however, the high reactivity of this four-membered ring leads to its susceptibility to non-selective hydrolysis in environmental media, generating eco-toxic ring-opening derivatives (e.g., phenylacetic acid metabolites). To address the above problems, researchers have developed a variety of targeted processing techniques. Wang et al. [127] designed a carbon quantum dot-functionalized molecularly imprinted polymer (CPDs-NH@MIP) whose surface-modified amino group and conjugated double bond can accurately recognize ceftiofur sodium molecules through multiple interactions (hydrogen bonding,  $\pi$ - $\pi$  stacking) and break through the spatial site resistance limitation of traditional adsorbents; an equilibrium adsorption of  $68.62 \text{ mg} \cdot \text{g}^{-1}$  with a selectivity coefficient of 5.61 was achieved in 10 min. In the field of catalytic degradation, Mehralipour's team [128] constructed rGO/Fe<sup>0</sup>/Fe<sub>3</sub>O<sub>4</sub>/TiO<sub>2</sub> nanocomposites with hierarchical porous structure by the sol-gel method, which showed a degradation rate of 96% of the penicillin solution of  $52 \text{ mg} \cdot \text{L}^{-1}$ , and the catalyst can be recovered by an applied magnetic field. Further, the TiO<sub>2</sub>/Bi<sub>2</sub>MoO<sub>6</sub> heterojunction photocatalyst constructed by Wang et al. [129] exhibited significantly enhanced photocatalytic performance during the degradation of amoxicillin, with reaction rate constants that were 18.2 and 5.7 times higher than those of pure TiO<sub>2</sub> and Bi<sub>2</sub>MoO<sub>6</sub>, respectively, which were attributed to the Z-type heterojunction-promoted directional mobility of the photogenerated carriers and the enhanced interfacial charge separation efficiency.

Table 6 summarizes the performance of MI-TiO<sub>2</sub> on five major antibiotics in marine wastewater. The excellent selectivity coefficients and degradation rates confirm that the precise matching between the imprinted cavities and the molecular structures of pollutants can effectively avoid the interference of the coexisting pollutants' competitive adsorption, which highlights the potential of the engineering application of MI-TiO<sub>2</sub> in complex marine environments.

**Table 6.** Comparison of MI-TiO<sub>2</sub> performance indices for five types of antibiotics.

Antibiotic Type	Antibiotic	Photocatalyst	Selectivity Factor	Degradation (%)	Reference
Tetracycline antibiotics	Tetracycline	MIP-TiO <sub>2</sub> @SiO <sub>2</sub>	-	82	[113]
	Oxytetracycline	MIP-Nd-TiO <sub>2</sub>	1.7	92	[53]
	Tetracycline	TMIP	3.4	100	[114]
	Oxytetracycline	TiO <sub>2</sub> /SiO <sub>2</sub> /OTC	-	81	[116]
Sulfonamide antibiotics	Sulfamethoxazole	MIP-TiO <sub>2</sub> /SMZ	4.0	99	[117]
	Sulfadiazine	MIP-TiO <sub>2</sub> /SD	1.3	95	[117]
	Sulfamethoxazole	MFTC	2.8	97	[119]
Quinolone antibiotics	Ciprofloxacin	CT-MI	3.2	86	[120]
	Norfloxacin	MIFTA	3.1	88	[122]
	Norfloxacin	MIPs	3.4	77	[123]
Macrolide antibiotics	Erythromycin	EMIP	2.6	80	[124]
	Azithromycin	CA-GO-TiO <sub>2</sub> /PTFE	-	80	[126]
$\beta$ -lactam antibiotics	Ceftiofur sodium	CPDs-NH@MIP	5.6	82	[127]
	Penicillin	rGO/Fe <sup>0</sup> /Fe <sub>3</sub> O <sub>4</sub> /TiO <sub>2</sub>	-	96	[128]
	Amoxicillin	TNBM-80	-	95	[129]

## 5. Conclusions and Outlook

Molecularly imprinted  $\text{TiO}_2$  (MI- $\text{TiO}_2$ ) exhibits high efficiency (>90%) and selectivity in the targeted degradation of marine antibiotic pollutants (such as sulfonamides and tetracyclines) by combining molecular imprinting technology (MIT) with the photocatalytic properties of  $\text{TiO}_2$ , and the convenient recovery of the catalyst is realized by magnetic field-assisted technology. However, its practical application still faces multiple challenges: the uniformity of imprinting sites and the efficiency of template elution need to be optimized in the industrial amplification process, and the mechanism of material stability and activity attenuation in long-term recycling needs to be analyzed. In addition, photocatalytic degradation may generate toxic intermediates (such as chlorinated or nitrified derivatives). It is necessary to clarify its environmental risks through LC-MS analysis and ecotoxicity assessment and to develop enhanced oxidation or biological synergistic processes to achieve complete mineralization. In terms of industrial scalability, the current synthesis cost is high (involving template molecule preparation, dopant introduction, etc.), and it is necessary to explore low-cost biomass templates and green synthesis routes to reduce large-scale production costs. The following recommendations can be made for future investigations:

- A photo-electro-magnetic synergistic catalytic system was constructed to improve the degradation efficiency and monitor the formation of by-products in real time to ensure environmental safety.
- Artificial intelligence is used to optimize the geometric configuration and doping strategy of imprinted cavities, so as to realize the efficient recognition and degradation of specific antibiotics.
- The long-term performance of MI- $\text{TiO}_2$  in complex environments was evaluated by establishing a test platform that simulated real marine conditions (such as dynamic salinity and biofouling).
- The full-cycle environmental footprint of MI- $\text{TiO}_2$  from synthesis to abandonment was systematically analyzed to promote the development of sustainable technology.

Through interdisciplinary technological innovation and large-scale engineering practice, MI- $\text{TiO}_2$  is expected to become an efficient, low-toxic, and recyclable core solution for marine pollution control, helping to achieve the synergistic goal of ecological restoration and sustainable development.

**Author Contributions:** Conceptualization, X.H. and Y.J.; methodology, B.R. and X.S.; software, Y.Z.; validation, Y.J. and L.Z.; investigation, X.S., R.L. and X.H.; resources, R.L.; data curation, B.R.; writing—original draft preparation, X.H. and Y.Z.; writing—review and editing, X.H.; visualization, B.R.; supervision, R.L. All authors have read and agreed to the published version of the manuscript.

**Funding:** This publication is based upon work supported by the Natural Science Foundation of China (No. 42207266); the Key Research and Development Plan of Heilongjiang Province (No. 2024ZXDXA49); and the Postdoctoral Funding Project of Heilongjiang Province (No. LBH-Z23261).

**Institutional Review Board Statement:** Not applicable.

**Informed Consent Statement:** Not applicable.

**Data Availability Statement:** No new data were created or analyzed in this study.

**Acknowledgments:** The authors thank the funding institution for support.

**Conflicts of Interest:** The authors declare no conflicts of interest.

## References

1. Yang, J.; Wang, S.; Luo, X.; Yu, Z.; Zhou, Y. Fenton-like process in antibiotic-containing wastewater treatment: Applications and toxicity evaluation. *Chin. Chem. Lett.* 2025, *in press*. [[CrossRef](#)]

2. WHO. Ten Threats to Global Health in 2019. Available online: <https://www.who.int/news-room/spotlight/ten-threats-to-global-health-in-2019> (accessed on 3 March 2025).
3. Anwar, M.; Iqbal, Q.; Saleem, F. Improper disposal of unused antibiotics: An often overlooked driver of antimicrobial resistance. *Expert. Rev. Anti-Infect. Ther.* **2020**, *18*, 697–699. [[CrossRef](#)] [[PubMed](#)]
4. Wang, P.; Wang, H.; Qi, S.; Wang, W.; Lu, H. Synergistic effects of quaternary ammonium compounds and antibiotics on the evolution of antibiotic resistance. *Water Res.* **2025**, *275*, 123206. [[CrossRef](#)]
5. Li, K.; Cheng, Y.; Chen, C.; Fan, Y.; Fang, M.; Li, X. Molecularly imprinted composite membranes with the dual imprinted network for highly selective separation of acteoside. *Sep. Purif. Technol.* **2025**, *358*, 130203. [[CrossRef](#)]
6. Lu, J.; Qin, Y.Y.; Wu, Y.L.; Zhu, Z.; Chen, M.N.; Yan, Y.S.; Li, C.X. Bio-synthesis of molecularly imprinted membrane with photo-regeneration availability for selective separation applications. *Mater. Today Chem.* **2022**, *24*, 100836. [[CrossRef](#)]
7. Liu, X.; Xu, C.; Wang, X. Incorporation of Hydroquinone in the Synthesis of Bi<sub>2</sub>Ti<sub>2</sub>O<sub>7</sub>-TiO<sub>2</sub> Contributes to Higher Efficiency of Hydroquinone Degradation: Preparation, Characterization, and Photocatalytic Mechanism. *Langmuir* **2024**, *40*, 19260–19269. [[CrossRef](#)] [[PubMed](#)]
8. Semra, A.; Seçkin, K.; Cem, E.; Adil, D. Molecularly Imprinted Polymer-Based Sensors for Protein Detection. *Polymers* **2023**, *15*, 629. [[CrossRef](#)]
9. Ye, X.; Ge, L.; Jiang, T.; Guo, H.; Chen, B.; Liu, C.; Hayashi, K. Fully Inkjet-Printed Chemiresistive Sensor Array Based on Molecularly Imprinted Sol-Gel Active Materials. *ACS Sens.* **2022**, *7*, 1819–1828. [[CrossRef](#)]
10. Yáñez-Sedeño, P.; Campuzano, S.; Pingarrón, J.M. Electrochemical sensors based on magnetic molecularly imprinted polymers: A review. *Anal. Chim. Acta* **2017**, *960*, 1–17. [[CrossRef](#)]
11. Ananya, K.; Apichai, P.; Opas, B. A magnetic molecularly imprinted polymer hierarchical composite adsorbent embedded with a zinc oxide carbon foam nanocomposite for the extraction of sulfonamides. *Microchem. J.* **2022**, *179*, 107443. [[CrossRef](#)]
12. Kamel, A.H.; Rabboh, H.S.M.A.; Hefnawy, A. Molecularly imprinted polymer-based electrochemical sensors for monitoring the persistent organic pollutants chlorophenols. *RSC Adv.* **2024**, *14*, 20163–20181. [[CrossRef](#)] [[PubMed](#)]
13. Su, L.-H.; Qian, H.-L.; Yang, C.; Wang, C.; Wang, Z.; Yan, X.-P. Surface imprinted-covalent organic frameworks for efficient solid-phase extraction of fluoroquinolones in food samples. *J. Hazard. Mater.* **2023**, *459*, 132031. [[CrossRef](#)]
14. Solmaz, N.; Kheibar, D.; Fereshteh, A.; Rouholah, Z. Red-emissive carbon nanostructure-anchored molecularly imprinted Er-BTC MOF: A biosensor for visual anthrax monitoring. *Analyst* **2023**, *148*, 3379–3391. [[CrossRef](#)]
15. Elisabetta, M.; Tiziano, D.G.; Stefano, M.; Martina, C.; Cosimino, M.; Giuseppe, B. Vapor-Phase Synthesis of Molecularly Imprinted Polymers on Nanostructured Materials at Room-Temperature. *Small* **2023**, *19*, 2302274. [[CrossRef](#)]
16. Sun, Y.; Bai, L.; Han, C.; Lv, X.; Sun, X.; Wang, T. Hybrid amino-functionalized TiO<sub>2</sub>/sodium lignosulfonate surface molecularly imprinted polymer for effective scavenging of methylene blue from wastewater. *J. Clean. Prod.* **2022**, *337*, 130457. [[CrossRef](#)]
17. Louros, V.L.; Silva, V.; Silva, C.P.; Calisto, V.; Otero, M.; Esteves, V.I.; Freitas, R.; Lima, D.L.D. Sulfadiazine's photodegradation using a novel magnetic and reusable carbon based photocatalyst: Photocatalytic efficiency and toxic impacts to marine bivalves. *J. Environ. Manag.* **2022**, *313*, 115030. [[CrossRef](#)] [[PubMed](#)]
18. Qin, D.; Wang, J.; Ge, C.; Lian, Z. Fast extraction of chloramphenicol from marine sediments by using magnetic molecularly imprinted nanoparticles. *Microchim. Acta* **2019**, *186*, 428. [[CrossRef](#)]
19. Zhao, C.; Suyamud, B.; Yuan, Y.; Ghosh, S.; Xu, X.; Hu, J. Effect of non-antibiotic factors on conjugative transfer of antibiotic resistance genes in aquaculture water. *J. Hazard. Mater.* **2025**, *483*, 136701. [[CrossRef](#)]
20. Li, S.; Zhou, X.; Liu, L.; Su, Z.; Zhao, J.; Zhang, J.; Cai, Z.; Peñuelas, J.; Huang, X. Plant Diversity Reduces the Risk of Antibiotic Resistance Genes in Agroecosystems. *Adv. Sci.* **2025**, *12*, 2410990. [[CrossRef](#)]
21. Peiravi, M.; Zafarnak, S.; Taghvaei, H. Design and fabrication of a microchannel plasma reactor for pharmaceutical wastewater treatment. *J. Water Process Eng.* **2025**, *70*, 107007. [[CrossRef](#)]
22. Nugraha, M.W.; Kim, S.; Roddick, F.; Xie, Z.; Fan, L. A review of the recent advancements in adsorption technology for removing antibiotics from hospital wastewater. *J. Water Process Eng.* **2025**, *70*, 106960. [[CrossRef](#)]
23. Burgos, J.; Gómez, G.; Leiva, A.M.; Vidal, G. Effects of combined antibiotics on the biomass stability and the occurrence of antibiotic-resistant bacteria in activated sludge used for domestic wastewater treatment. *J. Water Process Eng.* **2025**, *70*, 106966. [[CrossRef](#)]
24. Huang, J.; Huang, J.; Shu, X.; Cheng, X.; Yu, H.; Cao, Y.; Hu, Z.; Yu, J.C. A photocatalytic system for the Alleviation of ocean acidification and antibiotic pollution. *Sep. Purif. Technol.* **2025**, *362*, 131771. [[CrossRef](#)]
25. Kong, M.; Zhang, Y.; Ma, Y.; Fang, H.; Wang, W.; Shi, G.; Yan, Y.; Zhang, S. Antibiotics and antibiotic resistance change bacterial community compositions in marine sediments. *Environ. Res.* **2024**, *244*, 118005. [[CrossRef](#)]
26. Adenike, A.; Martine, B.; Thorsten, B.; Mariana, R.; Oliver, W. Usage of antibiotics in aquaculture and the impact on coastal waters. *Mar. Pollut. Bull.* **2023**, *188*, 114645. [[CrossRef](#)]
27. Chen, S.; Liu, D.; Zhang, Q.; Guo, P.; Ding, S.; Shen, J.; Zhu, K.; Lin, W. A Marine Antibiotic Kills Multidrug-Resistant Bacteria without Detectable High-Level Resistance. *ACS Infect. Dis.* **2021**, *7*, 884–893. [[CrossRef](#)] [[PubMed](#)]



28. Xu, N.; Qiu, D.; Zhang, Z.; Wang, Y.; Chen, B.; Zhang, Q.; Wang, T.; Hong, W.; Zhou, N.-Y.; Penuelas, J.; et al. A global atlas of marine antibiotic resistance genes and their expression. *Water Res.* **2023**, *244*, 120488. [\[CrossRef\]](#)
29. Zhang, R.; Kang, Y.; Zhang, R.; Han, M.; Zeng, W.; Wang, Y.; Yu, K.; Yang, Y. Occurrence, source, and the fate of antibiotics in mariculture ponds near the Maowei Sea, South China: Storm caused the increase of antibiotics usage. *Sci. Total Environ.* **2021**, *752*, 141882. [\[CrossRef\]](#)
30. Zheng, Q.; Zhang, R.; Wang, Y.; Pan, X.; Tang, J.; Zhang, G. Occurrence and distribution of antibiotics in the Beibu Gulf, China: Impacts of river discharge and aquaculture activities. *Mar. Environ. Res.* **2012**, *78*, 26–33. [\[CrossRef\]](#)
31. Chau, H.T.C.; Kadokami, K.; Duong, H.T.; Kong, L.; Nguyen, T.T.; Nguyen, T.Q.; Ito, Y. Occurrence of 1153 organic micropollutants in the aquatic environment of Vietnam. *Environ. Sci. Pollut. Res.* **2018**, *25*, 7147–7156. [\[CrossRef\]](#)
32. Riaz, L.; Mahmood, T.; Khalid, A.; Rashid, A.; Siddique, M.B.A.; Kamal, A.; Coyne, M.S. Fluoroquinolones (FQs) in the environment: A review on their abundance, sorption and toxicity in soil. *Chemosphere* **2018**, *191*, 704–720. [\[CrossRef\]](#) [\[PubMed\]](#)
33. Kemper, N. Veterinary antibiotics in the aquatic and terrestrial environment. *Ecol. Indic.* **2008**, *8*, 1–13. [\[CrossRef\]](#)
34. Xu, W.H.; Zhang, G.; Wai, O.W.H.; Zou, S.C.; Li, X.D. Transport and adsorption of antibiotics by marine sediments in a dynamic environment. *J. Soils Sediment.* **2009**, *9*, 364–373. [\[CrossRef\]](#)
35. Jiang, L.; Zhai, W.; Wang, J.; Li, G.; Zhou, Z.; Li, B.; Zhou, H. Antibiotics and antibiotic resistance genes in the water sources of the Wuhan stretch of the Yangtze River: Occurrence, distribution, and ecological risks. *Environ. Res.* **2023**, *239*, 117295. [\[CrossRef\]](#) [\[PubMed\]](#)
36. Biel-Maeso, M.; Baena-Nogueras, R.M.; Corada-Fernández, C.; Lara-Martín, P.A. Occurrence, distribution and environmental risk of pharmaceutically active compounds (PhACs) in coastal and ocean waters from the Gulf of Cadiz (SW Spain). *Sci. Total Environ.* **2018**, *612*, 649–659. [\[CrossRef\]](#)
37. Kim, S.-C.; Carlson, K. Temporal and spatial trends in the occurrence of human and veterinary antibiotics in aqueous and river sediment matrices. *Environ. Sci. Technol.* **2007**, *41*, 50–57. [\[CrossRef\]](#)
38. Ali, A.M.; Rønning, H.T.; Alarif, W.; Kallenborn, R.; Al-Lihaibi, S.S. Occurrence of pharmaceuticals and personal care products in effluent-dominated Saudi Arabian coastal waters of the Red Sea. *Chemosphere* **2017**, *175*, 505–513. [\[CrossRef\]](#)
39. Alygizakis, N.A.; Gago-Ferrero, P.; Borova, V.L.; Pavlidou, A.; Hatzianestis, I.; Thomaidis, N.S. Occurrence and spatial distribution of 158 pharmaceuticals, drugs of abuse and related metabolites in offshore seawater. *Sci. Total Environ.* **2016**, *541*, 1097–1105. [\[CrossRef\]](#)
40. He, K.; Hain, E.; Timm, A.; Tarnowski, M.; Blaney, L. Occurrence of antibiotics, estrogenic hormones, and UV-filters in water, sediment, and oyster tissue from the Chesapeake Bay. *Sci. Total Environ.* **2018**, *650*, 3101–3109. [\[CrossRef\]](#)
41. Chen, Y.; Yang, J.; Zeng, L.; Zhu, M. Recent progress on the removal of antibiotic pollutants using photocatalytic oxidation process. *Crit. Rev. Env. Sci. Technol.* **2022**, *52*, 1401–1448. [\[CrossRef\]](#)
42. Li, S.; Wu, Y.; Zheng, H.; Li, H.; Zheng, Y.; Nan, J.; Ma, J.; Nagarajan, D.; Chang, J.S. Antibiotics degradation by advanced oxidation process (AOPs): Recent advances in ecotoxicity and antibiotic-resistance genes induction of degradation products. *Chemosphere* **2023**, *311*, 136977. [\[CrossRef\]](#) [\[PubMed\]](#)
43. Nguyen, A.Q.; Nguyen, A.T.Q.; Nguyen, N.T.M.; Nguyen, A.D.; Bui, H.V.; Nguyen-Thanh, L.; Nguyen, M.N. Sorption of oxytetracycline to micro-sized colloids under concentrated salt solution: A perspective on terrestrial-to-ocean transfer of antibiotics. *Sci. Total Environ.* **2023**, *905*, 167005. [\[CrossRef\]](#) [\[PubMed\]](#)
44. Yuan, Q.; Qu, S.; Li, R.; Huo, Z.; Gao, Y.; Luo, Y. Degradation of antibiotics by electrochemical advanced oxidation processes (EAOPs): Performance, mechanisms, and perspectives. *Sci. Total Environ.* **2023**, *856*, 159092. [\[CrossRef\]](#)
45. Ma, L.; Yang, H.; Guan, L.; Liu, X.; Zhang, T. Risks of antibiotic resistance genes and antimicrobial resistance under chlorination disinfection with public health concerns. *Environ. Int.* **2022**, *158*, 106978. [\[CrossRef\]](#) [\[PubMed\]](#)
46. Tavasol, F.; Tabatabaie, T.; Ramavandi, B.; Amiri, F. Design a new photocatalyst of sea sediment/titanate to remove cephalixin antibiotic from aqueous media in the presence of sonication/ultraviolet/hydrogen peroxide: Pathway and mechanism for degradation. *Ultrason. Sonochem.* **2020**, *65*, 105062. [\[CrossRef\]](#)
47. Rana, S.; Kumar, A.; Dhiman, A.; Mola, G.T.; Sharma, G.; Lai, C.W. Recent advances in photocatalytic removal of sulfonamide pollutants from waste water by semiconductor heterojunctions: A review. *Mater. Today Chem.* **2023**, *30*, 101603. [\[CrossRef\]](#)
48. Sajini, T.; Gigimol, M.G.; Mathew, B. A brief overview of molecularly imprinted polymers supported on titanium dioxide matrices. *Mater. Today Chem.* **2019**, *11*, 283–295. [\[CrossRef\]](#)
49. Li, J.; Song, Y.; Wang, F.; Zhang, X.; Zhu, H.; Zou, H. Preparation of inorganic-framework molecularly imprinted TiO<sub>2</sub>/SiO<sub>2</sub> nanofibers by one-step electrospinning and their highly selective photodegradation. *Inorg. Chem. Front.* **2023**, *10*, 4456–4470. [\[CrossRef\]](#)
50. He, C.; Ma, J.; Xu, H.; Ge, C.; Lian, Z. Selective capture and determination of doxycycline in marine sediments by using magnetic imprinting dispersive solid-phase extraction coupled with high performance liquid chromatography. *Mar. Pollut. Bull.* **2022**, *184*, 114215. [\[CrossRef\]](#)



51. Li, Y.; Xie, J.; Situ, W.; Gao, Y.; Huang, X.; Zhou, W.; Li, J.; Song, X. Selective adsorption-photocatalytic synergistic breakdown of sulfamethazine in milk using loaded molecularly imprinted  $\text{Ag}_3\text{PO}_4/\text{TiO}_2$  films. *Food Chem.* **2025**, *467*, 142194. [\[CrossRef\]](#)
52. Zhang, H.; Li, Y.; He, W.; Xue, C.; Peng, W.; Liu, H.; Wang, W.; Shi, Z.; Dai, W.; Yuan, Z.; et al. The optical and electrical properties of  $\text{V}_2\text{O}_5\text{-TiO}_2/\text{PI}$  Nanocomposite film prepared by the Sol-Gel method. *Infrared Phys. Technol.* **2025**, *145*, 105719. [\[CrossRef\]](#)
53. Huang, Z.; Wang, B.; Liu, B.; Liu, X.; Zhu, L.; Wang, X. Study on the Degradation Performance of Novel Molecularly Imprinted Nd-TiO<sub>2</sub> for Oxytetracycline Hydrochloride. *Curr. Anal. Chem.* **2024**, *20*, e15734110319990. [\[CrossRef\]](#)
54. Ferreira, V.R.A.; Azenha, M.A.; Pereira, C.M.; Silva, A.F. Molecularly Imprinted Methyl-Modified Hollow TiO<sub>2</sub> Microspheres. *Molecules* **2022**, *27*, 8510. [\[CrossRef\]](#)
55. Yu, H.; Chen, Y.; Guo, H.; Ma, W.; Li, J.; Zhou, S.; Lin, S.; Yan, L.; Li, K. Preparation of Molecularly Imprinted Carbon Microspheres by One-Pot Hydrothermal Method and Their Adsorption Properties to Perfluorooctane Sulfonate. *Chin. J. Anal. Chem.* **2019**, *47*, 1776–1784. [\[CrossRef\]](#)
56. Xiong, X.; Li, C.; Yang, X.; Shu, Y.; Jin, D.; Zang, Y.; Shu, Y.; Xu, Q.; Hu, X. In situ grown TiO<sub>2</sub> nanorod arrays functionalized by molecularly imprinted polymers for salicylic acid recognition and detection. *J. Electroanal. Chem.* **2020**, *873*, 114394. [\[CrossRef\]](#)
57. Li, X.; Wang, J.; Li, M.; Jin, Y.; Gu, Z.; Liu, C.; Ogino, K. Fe-doped TiO<sub>2</sub>/SiO<sub>2</sub> nanofibrous membranes with surface molecular imprinted modification for selective photodegradation of 4-nitrophenol. *Chin. Chem. Lett.* **2018**, *29*, 527–530. [\[CrossRef\]](#)
58. Fu, X.; Wen, D.; Shi, Y.; Zhao, S. Fabrication of the mesoporous TiO<sub>2</sub> modified Eu-CN system for the adsorption of tetracycline antibiotics. *J. Mol. Struct.* **2025**, *1321*, 140077. [\[CrossRef\]](#)
59. Uthiravel, V.; Narayanamurthi, K.; Raja, V.; Anandhabasker, S.; Kuppusamy, K. Green synthesis and characterization of TiO<sub>2</sub> and Ag-doped TiO<sub>2</sub> nanoparticles for photocatalytic and antimicrobial applications. *Inorg. Chem. Commun.* **2024**, *170*, 113327. [\[CrossRef\]](#)
60. Kuang, K.; Chen, Y.; Li, Y.; Ji, Y.; Jia, N. N-doped TiO<sub>2</sub>/Ti<sub>3</sub>C<sub>2</sub>-driven self-photocatalytic molecularly imprinted ECL sensor for sensitive and steady detection of dexamethasone. *Biosens. Bioelectron.* **2024**, *247*, 115914. [\[CrossRef\]](#)
61. Qi, H.; Wang, H. Facile synthesis of Pr-doped molecularly imprinted TiO<sub>2</sub> mesocrystals with high preferential photocatalytic degradation performance. *Appl. Surf. Sci.* **2020**, *511*, 145607. [\[CrossRef\]](#)
62. Asadbeigi, N.; Givianrad, M.H.; Azar, P.A.; Saber-Tehrani, M. Synthesis, Characterization and Optimization of Highly Selective Molecularly Imprinted Ni and F Co-Doped TiO<sub>2</sub> Photocatalyst for Effective Removal and Photocatalytic Decomposition of Paracetamol. *J. Water Chem. Technol.* **2023**, *45*, 303–321. [\[CrossRef\]](#)
63. Rescigno, R.; Sacco, O.; Venditto, V.; Fusco, A.; Donnarumma, G.; Lettieri, M.; Fittipaldi, R.; Vaiano, V. Photocatalytic activity of P-doped TiO<sub>2</sub> photocatalyst. *Photochem. Photobiol. Sci.* **2023**, *22*, 1223–1231. [\[CrossRef\]](#)
64. Zhu, L.; Liu, X.; Wang, X.; Meng, X. Evaluation of photocatalytic selectivity of Ag/Zn modified molecularly imprinted TiO<sub>2</sub> by multiwavelength measurement. *Sci. Total Environ.* **2020**, *703*, 134732. [\[CrossRef\]](#)
65. Vo, T.L.N.; Dao, T.T.; Duong, A.T.; Bui, V.H.; Nguyen, V.H.; Nguyen, D.L.; Nguyen, D.C.; Nguyen, T.H.; Nguyen, H.T. Enhanced photocatalytic degradation of organic dyes using Ce-doped TiO<sub>2</sub> thin films. *J. Sol-Gel Sci. Technol.* **2023**, *108*, 423–434. [\[CrossRef\]](#)
66. Rahman, E.H.; Nair, P.S.; Shinoj, V.K.; Shaji, S.; Bunnell, A.; Jobson, N.; Philip, R.R. Enhanced photocatalytic degradation efficiency of TiO<sub>2</sub> nanotubes by potassium doping. *J. Mater. Sci. Mater. Electron.* **2025**, *36*, 236. [\[CrossRef\]](#)
67. Jaramillo-Fierro, X.; Leon, R. Effect of Doping TiO<sub>2</sub> NPs with Lanthanides (La, Ce and Eu) on the Adsorption and Photodegradation of Cyanide-A Comparative Study. *Nanomaterials* **2023**, *13*, 1068. [\[CrossRef\]](#)
68. Yadav, V.; Saini, V.K.; Sharma, H. How different dopants leads to difference in photocatalytic activity in doped TiO<sub>2</sub>? *Ceram. Int.* **2020**, *46*, 27308–27317. [\[CrossRef\]](#)
69. Akhiani, S.B.; Thatikonda, S.K.; Solanki, M.B.; Akhiani, T.; Gone, S.; Rathore, M.S. Photoluminescence and photocatalytic activity of sol gel synthesized Mg doped TiO<sub>2</sub> nanoparticles. *Inorg. Chem. Commun.* **2024**, *170*, 113294. [\[CrossRef\]](#)
70. Kavi, G.K.; Ravindran, B.; Ravichandran, K.; Thirumurugan, K.; Varshini, M.; Suvathi, S. Combined influence of vanadium doping and rGO composite partnering on the photocatalytic ability of TiO<sub>2</sub>. *Mater. Lett.* **2025**, *381*, 137767. [\[CrossRef\]](#)
71. Verma, V.; Singh, S.V. Augmentation of photocatalytic degradation of methylene blue dye using lanthanum and iodine Co-doped TiO<sub>2</sub> nanoparticles, their regeneration and reuse; and preliminary phytotoxicity studies for potential use of treated water. *J. Environ. Chem. Eng.* **2023**, *11*, 111339. [\[CrossRef\]](#)
72. Deng, Z.; Osuga, R.; Matsubara, M.; Kanie, K.; Muramatsu, A. Morphological effect of TiO<sub>2</sub> nanoparticles in TiO<sub>2</sub>/g-C<sub>3</sub>N<sub>4</sub> heterojunctions on photocatalytic dye degradation. *Chem. Lett.* **2024**, *53*, upae171. [\[CrossRef\]](#)
73. Lin, L.; Shi, L.; Liu, S.; He, J. Preparation of TiO<sub>2</sub> Grafted on Graphene and Study on their Photocatalytic Properties. *Int. J. Photoenergy* **2023**, *2023*, 8676430. [\[CrossRef\]](#)
74. Ye, M.; Pan, J.; Guo, Z.; Liu, X.; Chen, Y. Effect of ball milling process on the photocatalytic performance of CdS/TiO<sub>2</sub> composite. *Nanotechnol. Rev.* **2020**, *9*, 558–567. [\[CrossRef\]](#)
75. Qin, Z.; Chen, L.; Ma, R.; Tomovska, R.; Luo, X.; Xie, X.; Su, T.; Ji, H. TiO<sub>2</sub>/BiYO<sub>3</sub> composites for enhanced photocatalytic hydrogen production. *J. Alloys Compd.* **2020**, *836*, 155428. [\[CrossRef\]](#)

76. Alimard, P.; Gong, C.; Itskou, I.; Kafizas, A. Achieving high photocatalytic NO<sub>x</sub> removal activity using a Bi/BiOBr/TiO<sub>2</sub> composite photocatalyst. *Chemosphere* **2024**, *368*, 143728. [\[CrossRef\]](#)
77. Prabhakaran, P.K.; Balu, S.; Sridharan, G.; Ganapathy, D.; Sundramoorthy, A.K. Development of Eco-friendly CQDs/TiO<sub>2</sub> nanocomposite for enhanced photocatalytic degradation of methyl orange dye. *Eng. Res. Express* **2025**, *7*, 015002. [\[CrossRef\]](#)
78. Balagoutham, P.; Vallarasu, K.; Sampathkumar, V.; Anitha, R.; Vijayalakshmi, V. Synergistic photocatalytic activity of LaFeO<sub>3</sub>/TiO<sub>2</sub> nanocomposites for methylene blue degradation under UV Light. *J. Mater. Sci. Mater. Electron.* **2025**, *36*, 472. [\[CrossRef\]](#)
79. Arora, M.; Kaur, H. Effect of doping in TiO<sub>2</sub>/chitosan composite on adsorptive-photocatalytic removal of gallic acid from water. *Chemosphere* **2025**, *373*, 144122. [\[CrossRef\]](#)
80. He, J.; Hu, Z.; Zhu, X.; Liu, Z. Enhanced photocatalytic treatment of oilfield wastewater using TiO<sub>2</sub>/MoS<sub>2</sub> nanocomposites prepared via sol-gel and hydrothermal methods. *React. Kinet. Mech. Catal.* **2025**, *138*, 1153–1174. [\[CrossRef\]](#)
81. Li, Y.; Chen, S.; Wan, X.; Jiang, N.; Duan, W.; Lei, W.; Nan, Y.; Ding, D.; Xiao, G. Powering efficient dye degradation based on nanostructured FeOOH/TiO<sub>2</sub> composite with hydrophilic surfaces and unparalleled photocatalytic performance. *Ceram. Int.* **2025**, *51*, 14966–14973. [\[CrossRef\]](#)
82. Dong, R.; Lu, H.; Mei, W.; Tang, S.; Xu, J. Bi<sub>2</sub>O<sub>3</sub>-Modified Rice-Like Brookite TiO<sub>2</sub> for Enhancing the Photocatalytic Activity under Visible-Light Irradiation. *ChemistrySelect* **2025**, *10*, e202405403. [\[CrossRef\]](#)
83. Mohammed-Amine, E.; Kaltoum, B.; El Mountassir, E.M.; Abdelaziz, A.T.; Stephanie, R.; Stephanie, L.; Anne, P.; Pascal, W.W.C.; Alrashed, M.M.; Salah, R. Novel sol-gel synthesis of TiO<sub>2</sub>/BiPO<sub>4</sub> composite for enhanced photocatalytic degradation of carbamazepine under UV and visible light: Kinetic, identification of photoproducts and mechanistic insights. *J. Water Process Eng.* **2025**, *70*, 107098. [\[CrossRef\]](#)
84. Meirelles, R.M.; Giroto, A.S.; Furukawa, K.; Gonçalves, M. Valorization of Lignocellulosic Biomass for Photocatalytic Applications: Development of Activated Carbon-TiO<sub>2</sub> Composites. *ACS Sustain. Resour. Manag.* **2025**, *2*, 524–535. [\[CrossRef\]](#)
85. Yang, D.; Xia, Y.; Xiao, T.; Xu, Z.; Lei, Y.; Jiao, Y.; Zhu, X.; Feng, W. Constructing Ag-TiO<sub>2</sub>-g-C<sub>3</sub>N<sub>4</sub> S-scheme heterojunctions for photocatalytic degradation of malachite green. *Opt. Mater.* **2025**, *159*, 116652. [\[CrossRef\]](#)
86. Almutairi, S.T. Enhanced photocatalytic degradation of methylene blue using a ZnO-TiO<sub>2</sub>/rGO nanocomposite under UV irradiation. *Ionics* **2025**, *31*, 2789–2805. [\[CrossRef\]](#)
87. Liu, S.; Lou, H.; Luo, J.; Albashir, D.; Shi, Y.; Chen, Q. A Novel In Situ Biosynthesized Bacterial Cellulose/MoS<sub>2</sub>/TiO<sub>2</sub> Composite Film for Efficient Removal of Dyes and Pathogenic Bacteria from Industrial Wastewater under Sunlight Illumination. *ACS Appl. Mater. Interfaces* **2025**, *17*, 19453–19561. [\[CrossRef\]](#)
88. Appu, S.; Udayabhanu; Anusha, B.R.; Priyadarshini, H.N.; Alharethy, F.; Srinivas, R.G.; Abhijna; Nagaraju, G.; Prashantha, K. Type-1 heterojunction TiO<sub>2</sub> Nanotubes/Ag<sub>2</sub>CrO<sub>4</sub> nanoparticles: Advanced photocatalytic and electrochemical applications. *Mater. Chem. Phys.* **2025**, *337*, 130573. [\[CrossRef\]](#)
89. Wu, J.; Chen, C.; Lin, C.; Kumar, K.; Lu, Y.; Liou, S.Y.H.; Chen, S.; Wei, D.; Dong, C.; Chen, C. Improved photocatalytic efficacy of TiO<sub>2</sub> open nanotube arrays: A view by XAS. *Appl. Surf. Sci.* **2020**, *527*, 146844. [\[CrossRef\]](#)
90. Sharafudheen, S.B.; Vijayakumar, C.; Anjana, P.M.; Bindhu, M.R.; Alharbi, N.S.; Khaled, J.M.; Kadaikunnan, S.; Kakarla, R.R.; Aminabhavi, T.M. Biogenically synthesized porous TiO<sub>2</sub> nanostructures for advanced anti-bacterial, electrochemical, and photocatalytic applications. *J. Environ. Manag.* **2024**, *366*, 121728. [\[CrossRef\]](#)
91. Liu, L.; Xue, Z.; Gao, T.; Zhao, Q.; Sun, Y.; Wu, Y. Photocatalytic degradation performance of Ag-modified flexible TiO<sub>2</sub> nanofiber film. *Opt. Mater.* **2025**, *160*, 116720. [\[CrossRef\]](#)
92. Mendonca, T.A.P.; Nascimento, J.P.C.; Casagrande, G.A.; Vieira, N.C.S.; Goncalves, M. Ethylenediamine-modified activated carbon photocatalyst with the highest TiO<sub>2</sub> attachment/dispersion for improved photodegradation of sulfamethazine. *Mater. Chem. Phys.* **2024**, *318*, 129203. [\[CrossRef\]](#)
93. Wu, Y.; Zang, Y.; Xu, L.; Wang, J.; Jia, H.; Miao, F. Synthesis of functional conjugated microporous polymer/TiO<sub>2</sub> nanocomposites and the mechanism of the photocatalytic degradation of organic pollutants. *J. Mater. Sci.* **2021**, *56*, 7936–7950. [\[CrossRef\]](#)
94. Wang, H.; Hu, X.; Ma, Y.; Zhu, D.; Li, T.; Wang, J. Nitrate-group-grafting-induced assembly of rutile TiO<sub>2</sub> nanobundles for enhanced photocatalytic hydrogen evolution. *Chin. J. Catal.* **2020**, *41*, 95–102. [\[CrossRef\]](#)
95. Li, Z.; Li, H.; Wang, S.; Yang, F.; Zhou, W. Mesoporous black TiO<sub>2</sub>/MoS<sub>2</sub>/Cu<sub>2</sub>S hierarchical tandem heterojunctions toward optimized photothermal-photocatalytic fuel production. *Chem. Eng. J.* **2022**, *427*, 131830. [\[CrossRef\]](#)
96. Yang, J.; Wang, J.; Wang, G.; Wang, K.; Li, J.; Zhao, L. In situ irradiated XPS investigation on S-scheme TiO<sub>2</sub>/Bi<sub>2</sub>S<sub>3</sub> photocatalyst with high interfacial charge separation for highly efficient photothermal catalytic CO<sub>2</sub> reduction. *J. Mater. Sci. Technol.* **2024**, *189*, 86–95. [\[CrossRef\]](#)
97. Su, L.; Liu, X.; Xia, W.; Wu, B.; Li, C.; Xu, B.; Yang, B.; Xia, R.; Zhou, J.; Qian, J.; et al. Simultaneous photothermal and photocatalytic MOF- derived C/TiO<sub>2</sub> composites for high-efficiency solar driven purification of sewage. *J. Colloid Interface Sci.* **2023**, *650*, 613–621. [\[CrossRef\]](#)
98. Tang, Z.; Deng, X.; Chen, X.; Jiang, C.; Cai, L.; Guo, T. Ag<sub>2</sub>S/TiO<sub>2</sub> Z-scheme heterojunction under magnetic field: Enhanced photocatalytic degradation of tetracycline. *J. Alloys Compd.* **2025**, *1010*, 177752. [\[CrossRef\]](#)

99. Grzegorska, A.; Ofoegbu, J.C.; Cervera-Gabalda, L.; Gomez-Polo, C.; Sannino, D.; Zielinska-Jurek, A. Magnetically recyclable TiO<sub>2</sub>/MXene/MnFe<sub>2</sub>O<sub>4</sub> photocatalyst for enhanced peroxymonosulphate-assisted photocatalytic degradation of carbamazepine and ibuprofen under simulated solar light. *J. Environ. Chem. Eng.* **2023**, *11*, 110660. [\[CrossRef\]](#)
100. Gu, X.; Li, C.; Jiang, H.; Li, C.; Hu, Y. Synthesis of Z-scheme amorphous WO<sub>3</sub>-loaded TiO<sub>2</sub> photocatalyst for enhanced photocatalytic degradation of dichloromethane: Internal electric field and mechanism exploration. *J. Environ. Chem. Eng.* **2024**, *12*, 113827. [\[CrossRef\]](#)
101. Riedel, R.; Schowarte, J.; Semisch, L.; Gonzalez-Castano, M.; Ivanova, S.; Arellano-Garcia, H.; Martienssen, M. Improving the photocatalytic degradation of EDTMP: Effect of doped NPs (Na, Y, and K) into the lattice of modified Au/TiO<sub>2</sub> nano-catalysts. *Chem. Eng. J.* **2025**, *506*, 160109. [\[CrossRef\]](#)
102. Fu, W.; Wang, S.; Zhang, Y.; Cheng, B.; Wu, Y. 2D/2D F-doped TiO<sub>2</sub>/CdS S-scheme heterojunction photocatalyst for enhanced photocatalytic H<sub>2</sub> generation. *J. Mater. Sci. Technol.* **2025**, *232*, 181–190. [\[CrossRef\]](#)
103. Lin, Z.; Pei, L.; Liu, S.; Jiang, X.; Xu, W.; Li, F.; Wu, X.; Wang, H.; Lu, X. Developments and challenges on crystal forms and morphologies of nano-TiO<sub>2</sub> photocatalysts in air and wastewater treatment. *J. Water Process Eng.* **2025**, *70*, 106909. [\[CrossRef\]](#)
104. Chhabria, D.; Sundaram, G.A.; Ganapathy, D.; Balasubramanian, P. Unveiling the biomedical and photocatalytic properties of copper(II) imidazole complex-functionalized TiO<sub>2</sub> nanoparticles. *J. Mol. Liq.* **2025**, *426*, 127368. [\[CrossRef\]](#)
105. Hosseini, S.F.; Dorraji, M.S.S.; Mohajer, S.; Saeedi, S.N.; Kianfar, M.; Koshelev, A.V.; Arkharova, N.A.; Karimov, D.N. Synergistic photothermal conversion and visible-light photodegradation of antibiotic in S-type TiO<sub>2</sub> derived Ti<sub>3</sub>C<sub>2</sub>-MXene loaded on NaYF<sub>4</sub>: Tm<sup>3+</sup>, Er<sup>3+</sup>, Yb<sup>3+</sup> @BiOI. *J. Sci. Adv. Mater. Devices* **2025**, *10*, 100851. [\[CrossRef\]](#)
106. Yee, L.Y.; Ng, Q.H.; Ab Rahim, S.K.; Hoo, P.Y.; Chang, P.T.; Ahmad, A.L.; Low, S.C.; Shuit, S.H. A Novel Tri-Functionality pH-Magnetic-Photocatalytic Hybrid Organic-Inorganic Polyoxometalates Augmented Microspheres for Polluted Water Treatment. *Membranes* **2023**, *13*, 174. [\[CrossRef\]](#) [\[PubMed\]](#)
107. Xu, W.; Zhang, C.; Wan, J.; Zhang, X.; Cheng, Y.; Jin, J.; Zhang, H.; Duan, C.; Fang, Y. Study on the matching of adsorption rate and photocatalytic rate under electric field synergy to enhance the degradation performance of cyclohexane. *Chem. Eng. Res. Des.* **2025**, *215*, 386–397. [\[CrossRef\]](#)
108. Shen, Y.; Li, J.; Chen, Z.; Wang, C.; Li, S.; Gui, D.; Zhu, X. Dye-encapsulated metal-organic frameworks as highly sensitive fluorescent sensors for tetracycline antibiotics in water. *Mater. Lett.* **2024**, *363*, 136243. [\[CrossRef\]](#)
109. Wang, L.; Li, J.; Du, Z.; Jin, M.; Yao, J.; Zhang, Z. MnFe<sub>2</sub>O<sub>4</sub>/zeolite composite catalyst for activating peroxymonosulfate to efficiently degrade antibiotic. *Mater. Lett.* **2023**, *344*, 134460. [\[CrossRef\]](#)
110. Lou, Z.; Wen, X.; Song, L.; Yan, C.; Chen, H.; Lu, T.; Yu, J.; Xu, X.; Li, J. Oxygen vacancy engineered molecular imprinted TiO<sub>2</sub> for preferential florfenicol remediation by electro-reductive approach: Enhanced dehalogenation performance and elimination of antibiotic resistance genes. *Appl. Catal. B Environ.* **2023**, *336*, 122923. [\[CrossRef\]](#)
111. Chen, X.; Li, Q.; Yuan, T.; Ma, M.; Ye, Z.; Wei, X.; Fang, X.; Mao, S. Highly Specific Antibiotic Detection on Water-Stable Black Phosphorus Field-Effect Transistors. *Acs Sens.* **2023**, *8*, 858–866. [\[CrossRef\]](#)
112. Do, T.C.M.V.; Nguyen, D.Q.; Nguyen, K.T.; Le, P.H. TiO<sub>2</sub> and Au-TiO<sub>2</sub> Nanomaterials for Rapid Photocatalytic Degradation of Antibiotic Residues in Aquaculture Wastewater. *Materials* **2019**, *12*, 2434. [\[CrossRef\]](#)
113. Li, Z.; Li, X.; Xu, S.; Tian, H.; Wang, C. Efficient identification and degradation of tetracycline hydrochloride from water by molecularly imprinted core-shell structured SiO<sub>2</sub>@TiO<sub>2</sub>. *New J. Chem.* **2023**, *47*, 13106–13116. [\[CrossRef\]](#)
114. Fu, J.; Li, S.; Li, Q.; Bell, E.; Yang, D.; Li, T.; Li, Y.; He, J.; Zhou, L.; Zhang, Q.; et al. Preparation of surface molecular-imprinted MOFs for selective degradation of tetracycline antibiotics in wastewater. *Colloids Surf. A Physicochem. Eng. Asp.* **2024**, *687*, 133575. [\[CrossRef\]](#)
115. Fu, J.; Yu, X.; Li, Z.; Zhang, Y.; Zhu, W.; Liu, J. Study on the Degradation of Chlortetracycline Hydrochloride in Mariculture Wastewater by Zn<sub>0.75</sub>Mn<sub>0.75</sub>Fe<sub>1.5</sub>O<sub>4</sub>/ZnFe<sub>2</sub>O<sub>4</sub>/ZnO Photocatalyst. *Water Air Soil Pollut.* **2021**, *232*, 12. [\[CrossRef\]](#)
116. Guo, J.; Li, S.; Duan, L.; Guo, P.; Li, X.; Cui, Q.; Wang, H.; Jiang, Q. Preparation of Si doped molecularly imprinted TiO<sub>2</sub> photocatalyst and its degradation to antibiotic wastewater. *Integr. Ferroelectr.* **2016**, *168*, 170–182. [\[CrossRef\]](#)
117. Li, D.; Yuan, R.; Zhou, B.; Chen, H. Selective photocatalytic removal of sulfonamide antibiotics: The performance differences in molecularly imprinted TiO<sub>2</sub> synthesized using four template molecules. *J. Clean. Prod.* **2023**, *383*, 135470. [\[CrossRef\]](#)
118. Wang, C.; Zhan, Z.; Liu, H.; Li, Y.; Wu, J.; Sun, P.; Shen, G. Single-atom iron cocatalyst for highly enhancing TiO<sub>2</sub> photocatalytic degradation of antibiotics and antibiotic-resistant genes. *Chem. Eng. J.* **2024**, *482*, 148906. [\[CrossRef\]](#)
119. Zhang, J.; Ding, J.; Liu, L.; Wu, R.; Ding, L.; Jiang, J.; Pang, J.; Li, Y.; Ren, N.; Yang, S. Selective removal of sulfamethoxazole by a novel double Z-scheme photocatalyst: Preferential recognition and degradation mechanism. *Environ. Sci. Ecotechnol.* **2024**, *17*, 100308. [\[CrossRef\]](#) [\[PubMed\]](#)
120. Li, L.; Zheng, X.; Chi, Y.; Wang, Y.; Sun, X.; Yue, Q.; Gao, B.; Xu, S. Molecularly imprinted carbon nanosheets supported TiO<sub>2</sub>: Strong selectivity and synergic adsorption-photocatalysis for antibiotics removal. *J. Hazard. Mater.* **2020**, *383*, 121211. [\[CrossRef\]](#)
121. Qin, D.; Zhao, M.; Wang, J.; Lian, Z. Selective extraction and detection of norfloxacin from marine sediment and seawater samples using molecularly imprinted silica sorbents coupled with HPLC. *Mar. Pollut. Bull.* **2020**, *150*, 110677. [\[CrossRef\]](#)

122. Zheng, L.; Liao, W.; Wu, J.; Long, Q.; Luo, Y.; Li, X.; Huang, L.; Jia, L.; Li, H.; Liu, K. Selective adsorption and photodegradation of residual norfloxacin in water using a mTiO<sub>2</sub> based inorganic molecularly imprinted magnetic photocatalyst. *New J. Chem.* **2024**, *48*, 15567–15576. [[CrossRef](#)]
123. Li, S.; Fang, L.; Ye, M.; Zhang, Y. Enhanced adsorption of norfloxacin on modified TiO<sub>2</sub> particles prepared via surface molecular imprinting technique. *Desalination Water Treat.* **2016**, *57*, 408–418. [[CrossRef](#)]
124. Xie, W.; Wu, Y.; Yan, W.; Ma, Y.; Meng, H.; Wang, G.; Zhang, L.; Jia, G.; Li, W.; Xiao, Y.; et al. The erythromycin sorption removal at environmentally relevant concentration based on molecular imprinted polymer: Performance and mechanism. *Environ. Pollut.* **2023**, *336*, 122425. [[CrossRef](#)]
125. Cizmic, M.; Ljubas, D.; Rozman, M.; Asperger, D.; Curkovic, L.; Babic, S. Photocatalytic Degradation of Azithromycin by Nanostructured TiO<sub>2</sub> Film: Kinetics, Degradation Products, and Toxicity. *Materials* **2019**, *12*, 873. [[CrossRef](#)] [[PubMed](#)]
126. Satulu, V.; Pandele, A.M.; Ionica, G.I.; Bobirica, L.; Bonciu, A.F.; Scarlatescu, A.; Bobirica, C.; Orbeci, C.; Voicu, S.I.; Mitu, B.; et al. Robust CA-GO-TiO<sub>2</sub>/PTFE Photocatalytic Membranes for the Degradation of the Azithromycin Formulation from Wastewaters. *Polymers* **2024**, *16*, 1368. [[CrossRef](#)]
127. Wang, L.; Liu, L.; Chen, R.; Jiao, Y.; Zhao, K.; Liu, Y.; Zhu, G. Carbonized polymer dots-based molecular imprinting: An adsorbent with enhanced selectivity for highly efficient recognition and removal of ceftiofur sodium from complex samples. *J. Hazard. Mater.* **2024**, *473*, 134637. [[CrossRef](#)]
128. Mehralipour, J.; Bagheri, S.; Gholami, M. Synthesis and characterization of rGO/Fe<sup>0</sup>/Fe<sub>3</sub>O<sub>4</sub>/TiO<sub>2</sub> nanocomposite and application of photocatalytic process in the decomposition of penicillin G from aqueous. *Heliyon* **2023**, *9*, e18172. [[CrossRef](#)]
129. Wang, Y.; Zuo, G.; Kong, J.; Guo, Y.; Xian, Z.; Dai, Y.; Wang, J.; Gong, T.; Sun, C.; Xian, Q. Sheet-on-sheet TiO<sub>2</sub>/Bi<sub>2</sub>MoO<sub>6</sub> heterostructure for enhanced photocatalytic amoxicillin degradation. *J. Hazard. Mater.* **2022**, *421*, 126634. [[CrossRef](#)]

**Disclaimer/Publisher's Note:** The statements, opinions and data contained in all publications are solely those of the individual author(s) and contributor(s) and not of MDPI and/or the editor(s). MDPI and/or the editor(s) disclaim responsibility for any injury to people or property resulting from any ideas, methods, instructions or products referred to in the content.